

# iPhones and Dysons: Using fluid dynamics to tailor technology

Ian Griffiths

Mathematical Institute, University of Oxford  
Department of Mathematics, Princeton University



# Bangladesh

[Latest](#)

## Providing safe water for families in Bangladesh

### › Newsline

[Statistics](#)[Contact us](#)[Country website](#)**By Naimul Haq**

BAGERHAT DISTRICT, Bangladesh, 24 February 2010 — Defying stifling heat and humidity, Maya Begum walks more than an hour from her village to fill two large plastic containers with drinking water for her family of four.

# The INDEPENDENT

## Arsenic-tainted water from Unicef wells is poisoning half of Bangladesh

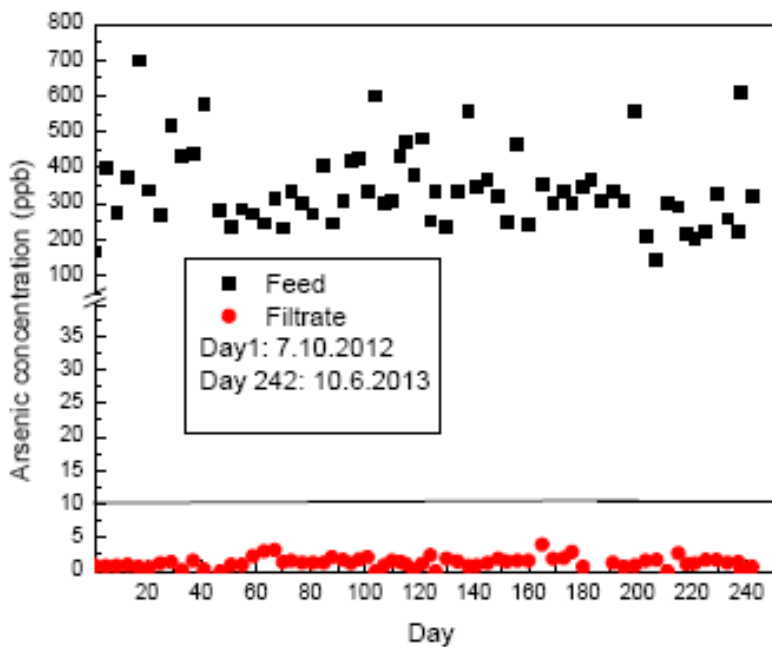
PETER POPHAM IN DHAKA | Saturday 05 September 1998



Karagas, *The Lancet*, 2010

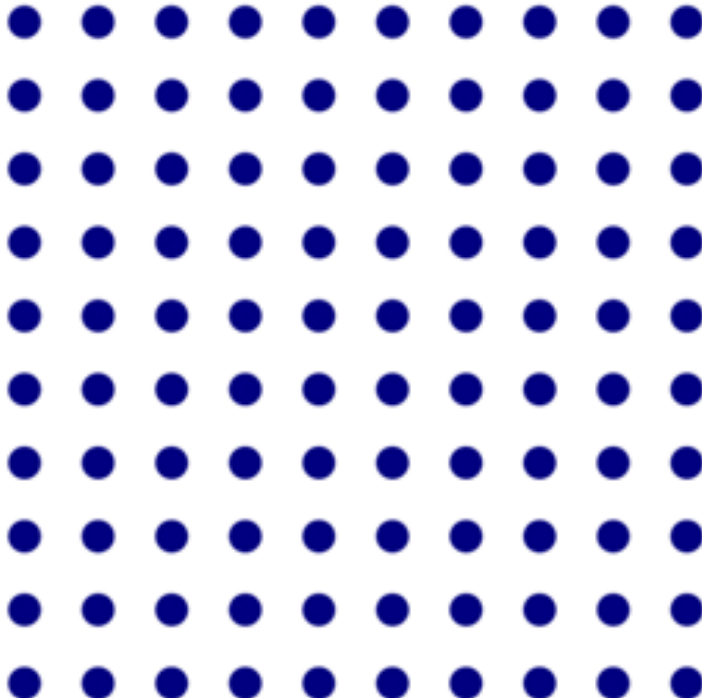
# A strategy for arsenic removal?

- Iron-rich laterite soil removes arsenic.



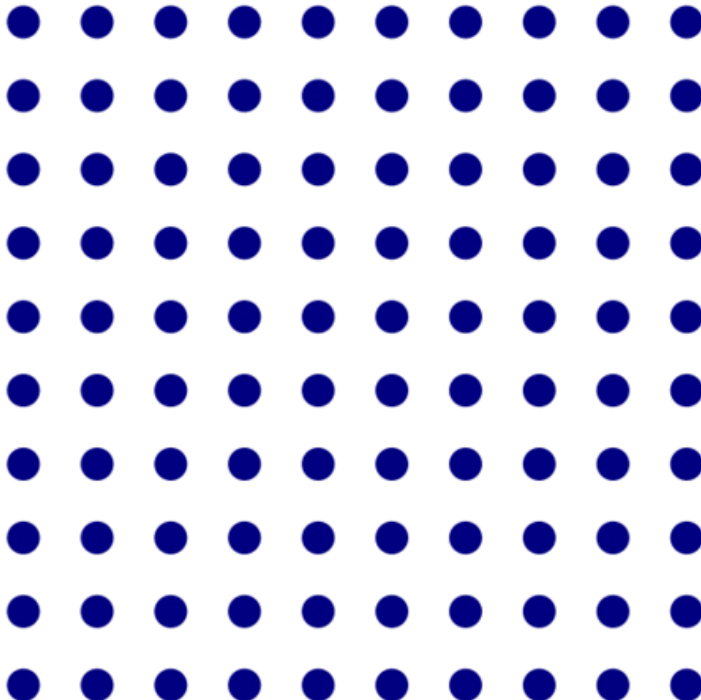
# *Modelling particle removal*

- We can simulate the transport and adhesion of contaminants as they pass through the filter using our custom-designed software *Aboria*:



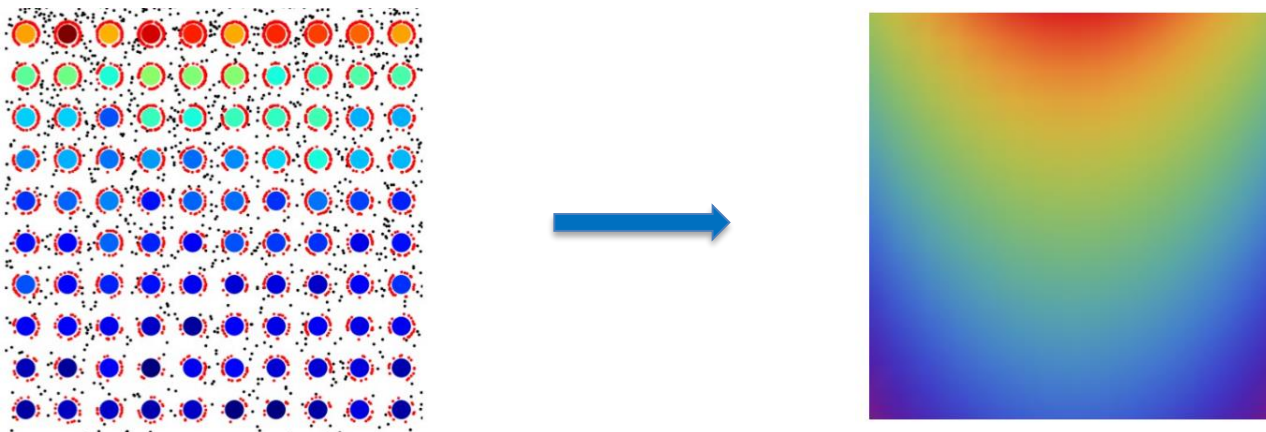
# *Modelling particle removal*

- We can simulate the transport and adhesion of contaminants as they pass through the filter using our custom-designed software *Aboria*:

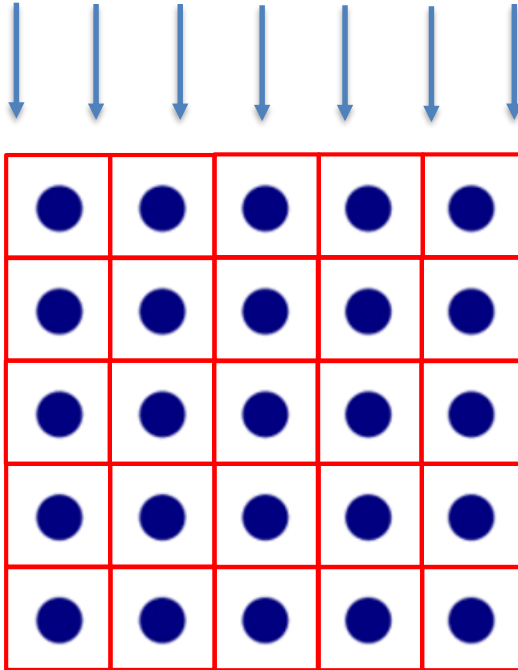


# *Modelling particle removal*

- Homogenization theory allows us to write down a macroscale description that captures the microscale behaviour:



# Modelling particle removal



- Solve for the flow in a single unit cell to obtain a net diffusivity,  $\tilde{D}$ , and permeability,  $\tilde{\mathcal{K}}$ .
- Use the method of multiple scales to obtain effective macroscale equations for the velocity,  $\mathbf{u}$ , pressure,  $p$ , and contaminant concentration,  $c$ :

$$\nabla \cdot \mathbf{u} = 0$$

$$\mathbf{u} = -\tilde{\mathcal{K}} \nabla p$$

$$\frac{\partial c}{\partial t} + \mathbf{u} \cdot \nabla c = \nabla \left( \tilde{D} \nabla c \right)$$

# *Modelling particle removal*

- Contaminant particles are removed from the fluid by **adsorbing** to the soil.

$$\frac{\partial c}{\partial t} + \mathbf{u} \cdot \nabla c = \nabla \left( \tilde{D} \nabla c \right) - \tilde{k}c(q_{max} - q)$$

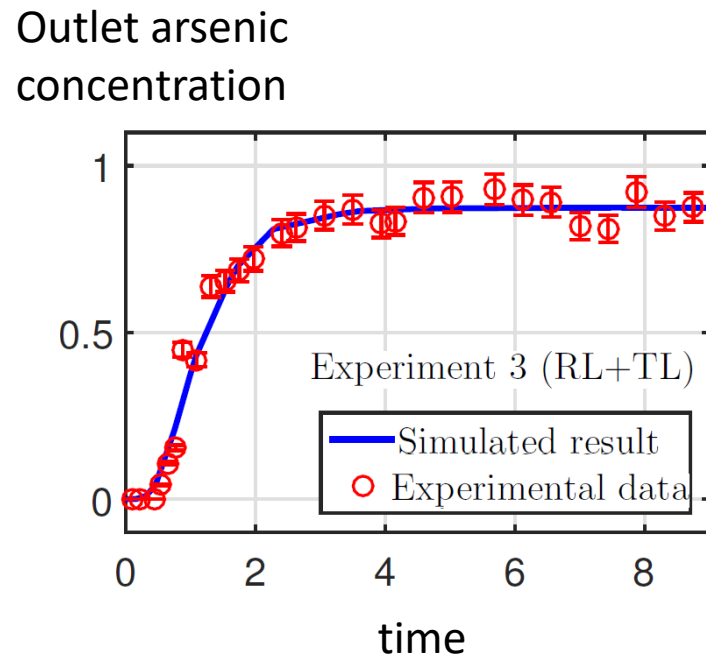
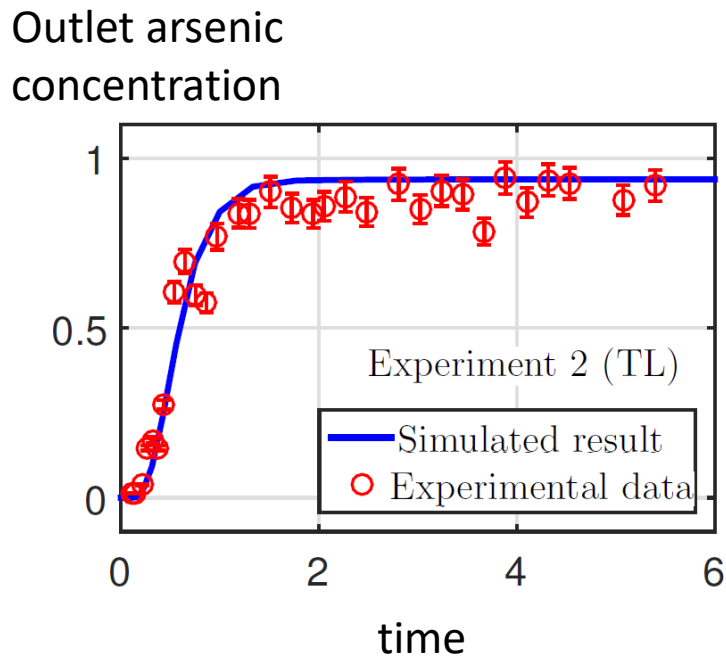
  
adsorbed  
contaminant  
concentration

- Conservation of mass determines  $q$ :

$$\frac{\partial q}{\partial t} = \tilde{k}c(q_{max} - q)$$

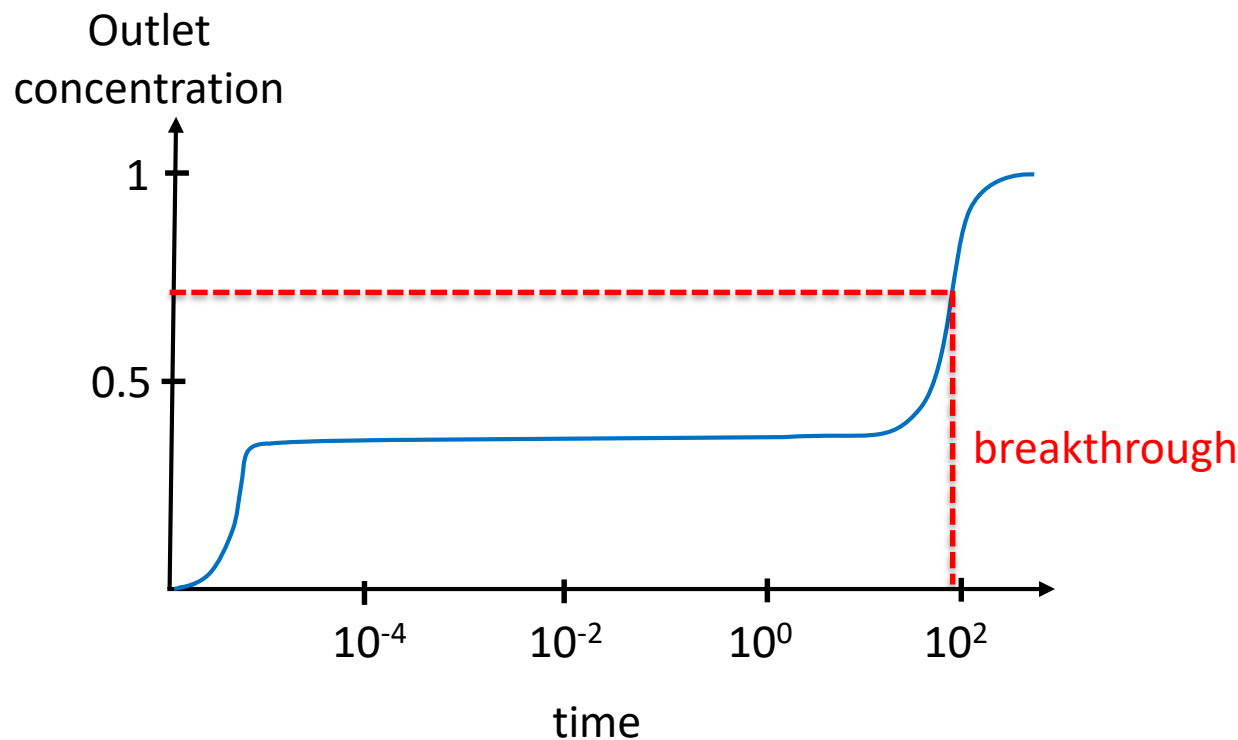
# Modelling particle removal

- We use experiments to validate our theory for **small experiments** and **short times**:



# *Modelling particle removal*

- The theory can then be used to determine the behaviour for **larger filters** over **longer times**:



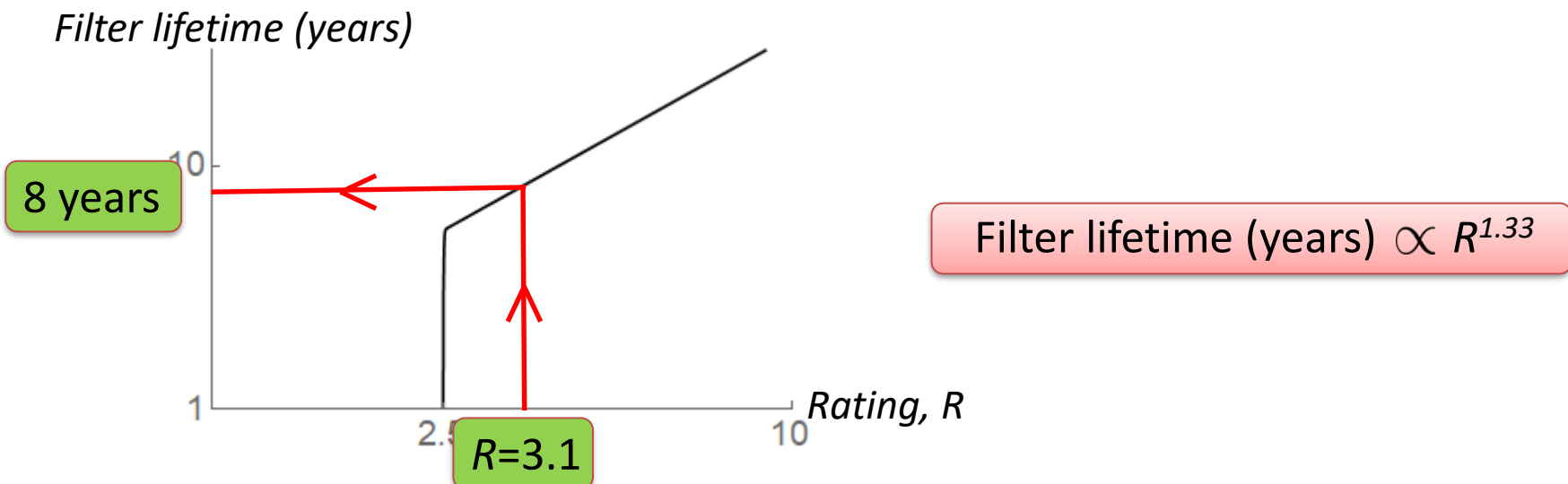
# Using the results

- The homogenized model captures the filter behaviour in terms of a single design parameter, **the filter rating  $R$** :

$$R = \frac{Mk}{Q}$$

$M$  = Mass of soil (kg),  
 $k$  = Adsorption rate ( $s^{-1}$ )  
 $Q$  = required filter flow rate ( $\text{kg s}^{-1}$ )

- We obtain a simple formula for when a given filter must be replaced:



# *State of deployment*



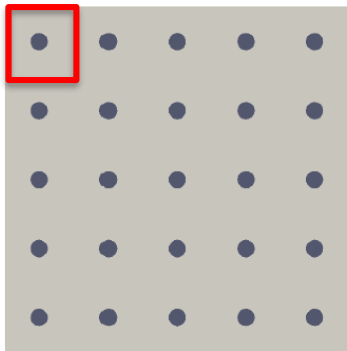
Ambika Soudamini school 1500 litres per day



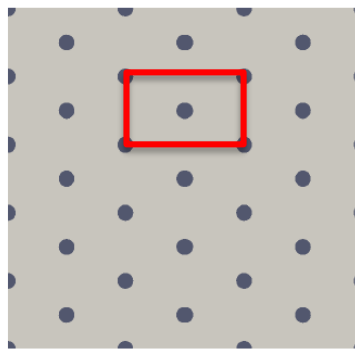
Dutta Pukur 2000 litres per hour

*But real filter media isn't regularly arranged*

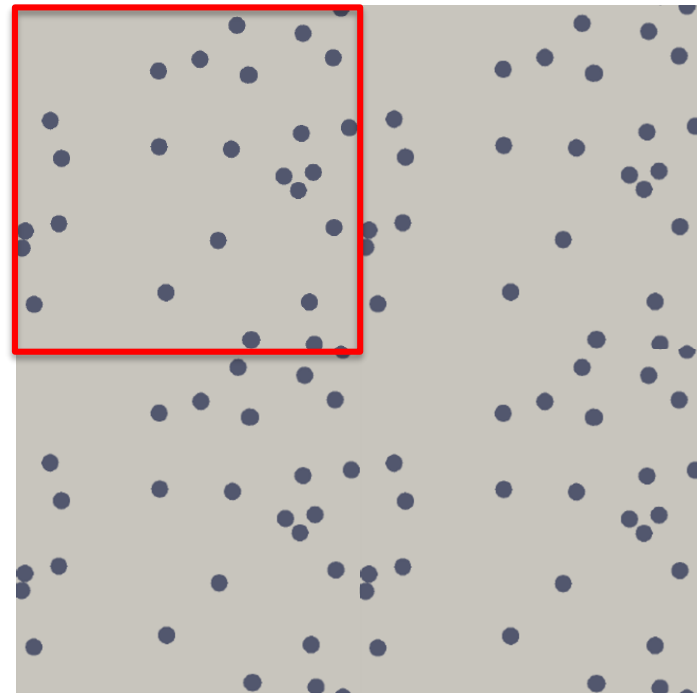
Square



Hexagonal

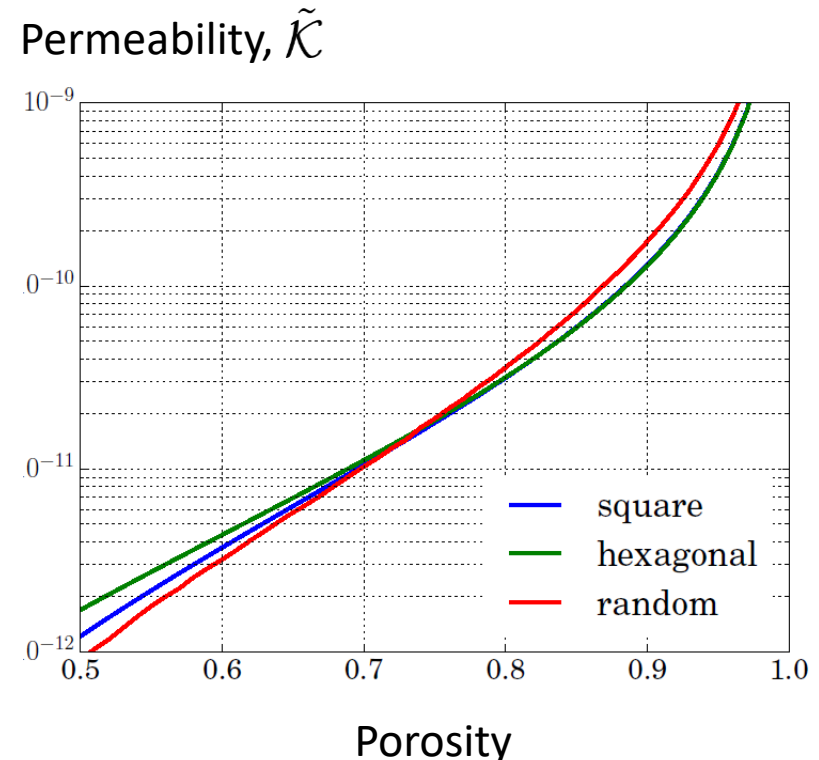
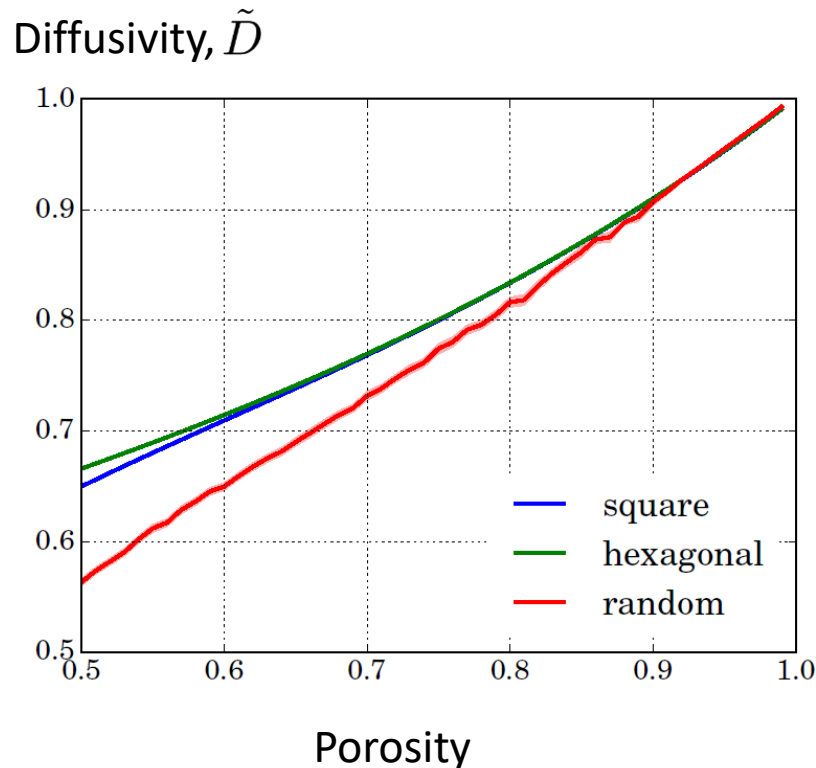


Random



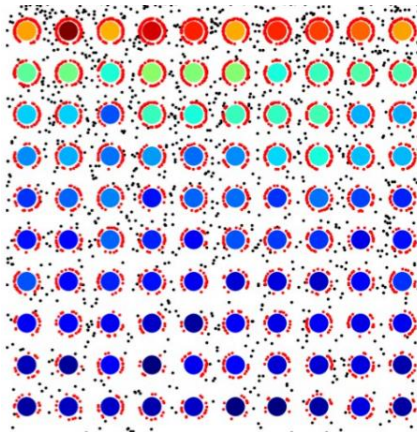
# *The effect of microstructure arrangement*

- The microstructure changes the **diffusivity** and **permeability**:



# *Improving filters*

- A higher proportion of contaminant adsorbs to obstacles closer to the inlet:



- This behaviour is generic among filters:



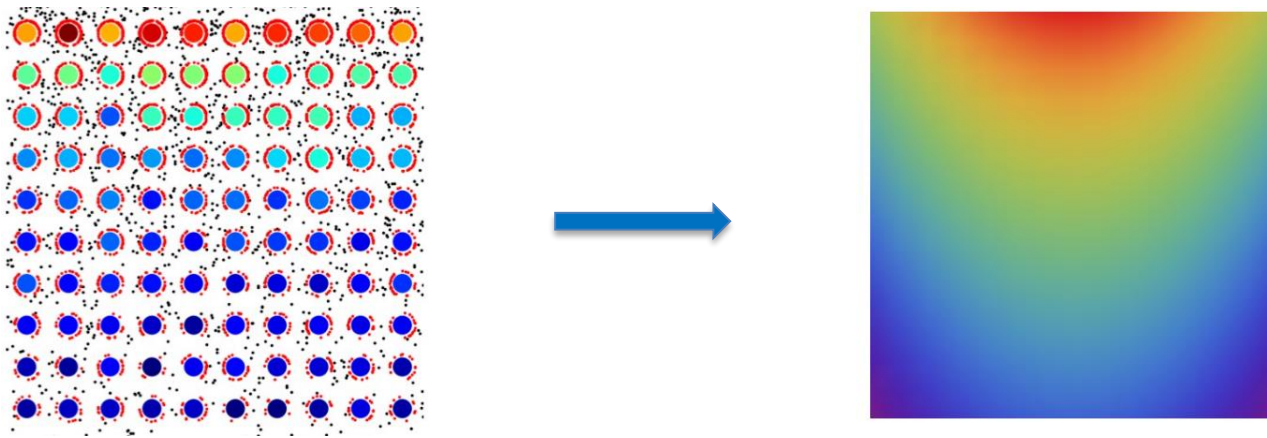
- The filter is not performing at its best.
- Could a **porosity graded filter** offer a solution?

*Oxford, England*

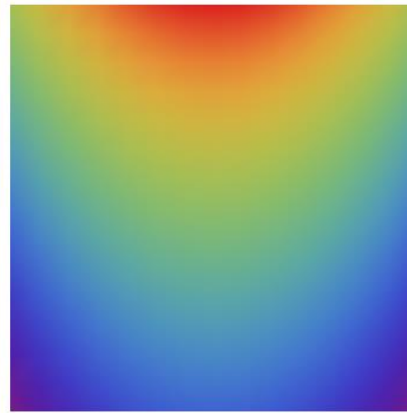
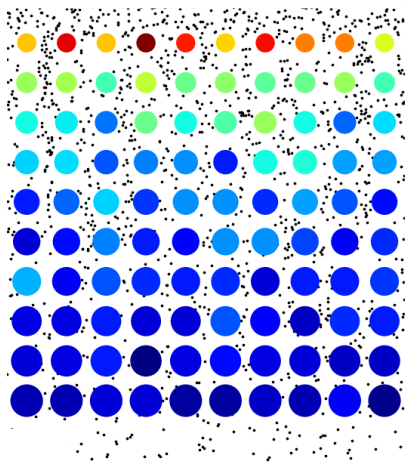


dyson

# *Porosity graded filters*



# *Porosity graded filters*

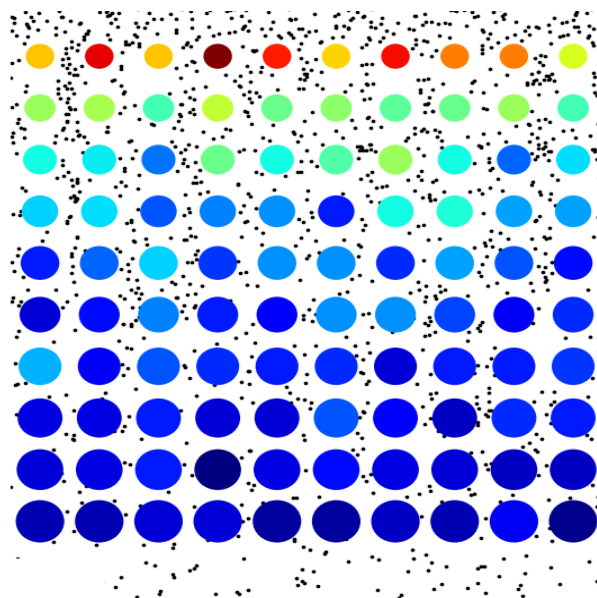


# *A porosity graded filter*

- We perform a similar technique to obtain a **macroscale master equation** for a **porosity graded filter** in terms of the porosity,  $\phi$

$$\frac{\partial c}{\partial t} = \nabla \left( \tilde{D}(\phi) \nabla c - \tilde{\mathbf{u}}(\phi) c + (\tilde{A}(\phi) \nabla \phi) c \right) - \tilde{k}(\phi)$$

$$\mathbf{u} = -\tilde{\mathcal{K}}(\phi) \nabla p$$

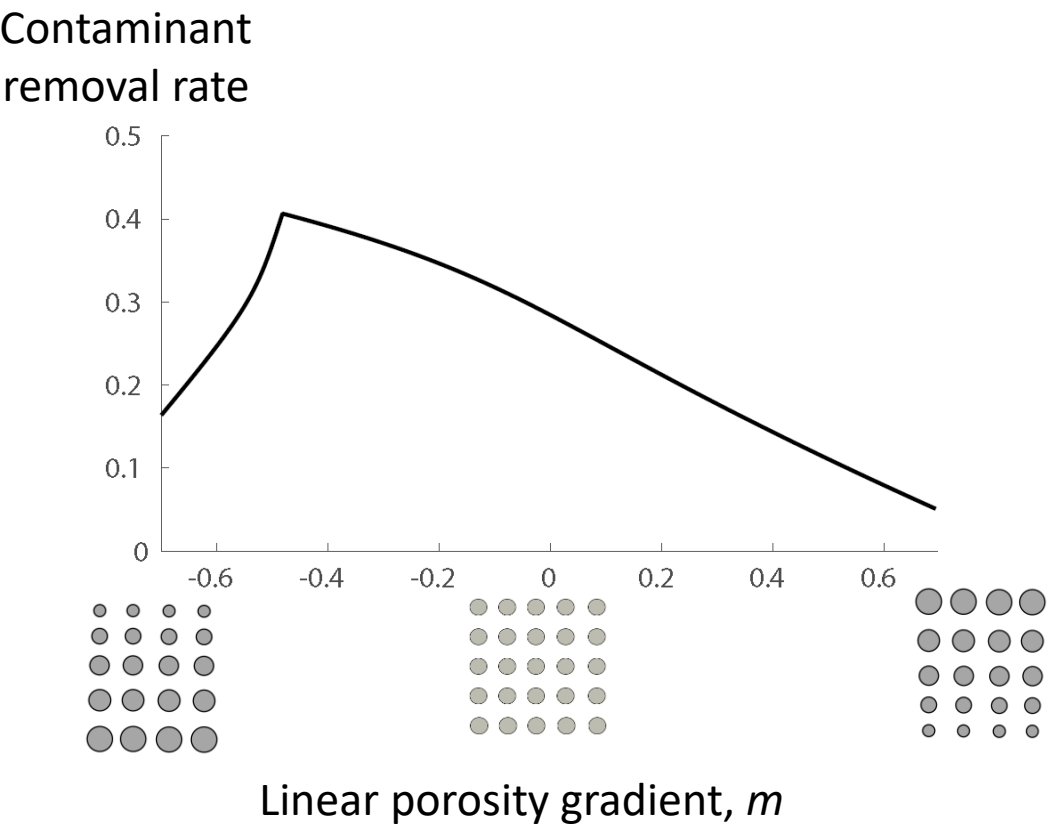


# Filter efficiency

- We consider a **constant porosity gradient**.

$$\phi = \phi_0 + m(x - 1/2)$$

- An **optimum constant porosity gradient,  $m$** , maximizes the total contaminant removal rate:



- So a **filter whose porosity decreases with depth remove more contaminants**.

# *Capturing filter blocking*

- What happens if the contaminants are larger and cause **blocking**?
- We solve the same macroscale master equation

$$\frac{\partial c}{\partial t} = \nabla \left( \tilde{D}(\phi) \nabla c - \mathbf{u}(\phi) c + (\tilde{A}(\phi) \nabla \phi) c \right) - \tilde{k}(\phi)$$

but now the **obstacle radii grow due to the particle adsorption**:

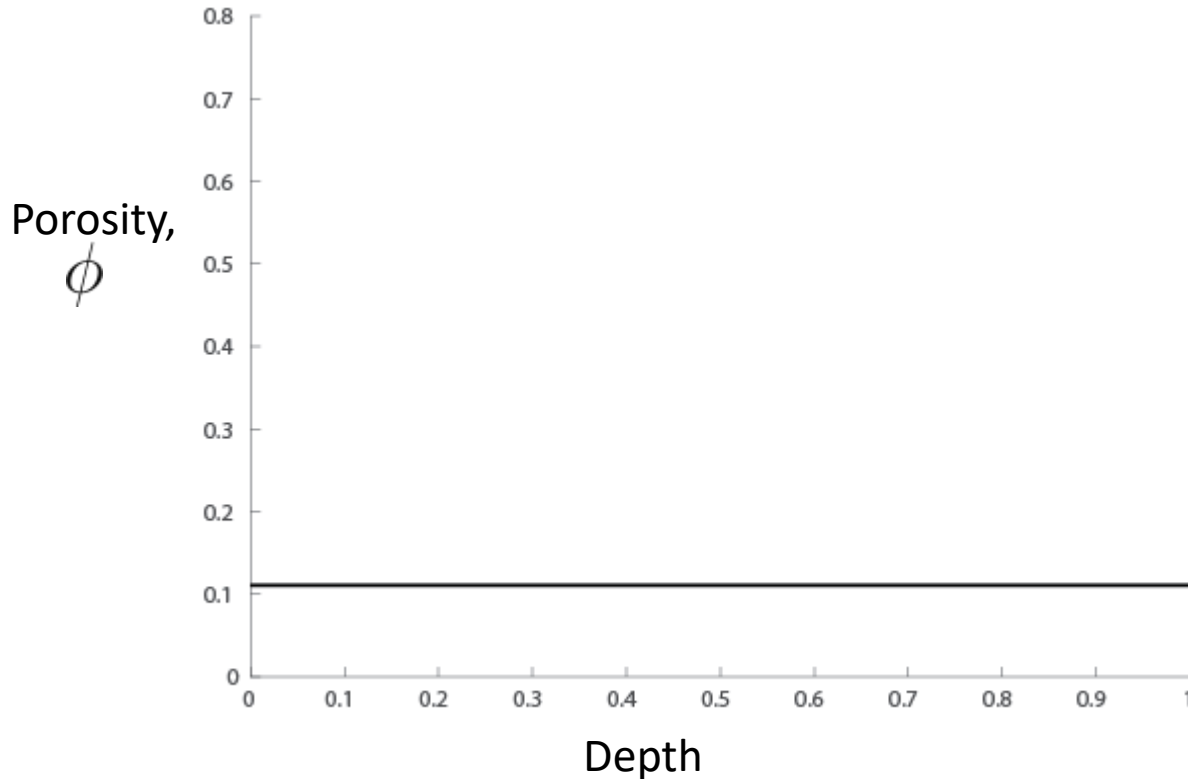
$$\frac{\partial R}{\partial t} = -\beta \frac{\partial c(R, t)}{\partial r}$$

which in turn **changes the flow field**:

$$\mathbf{u} = -\tilde{\mathcal{K}} \nabla p$$

# The filter that traps the most contaminant

- A filter that traps the most contaminant will **block everywhere at once**.



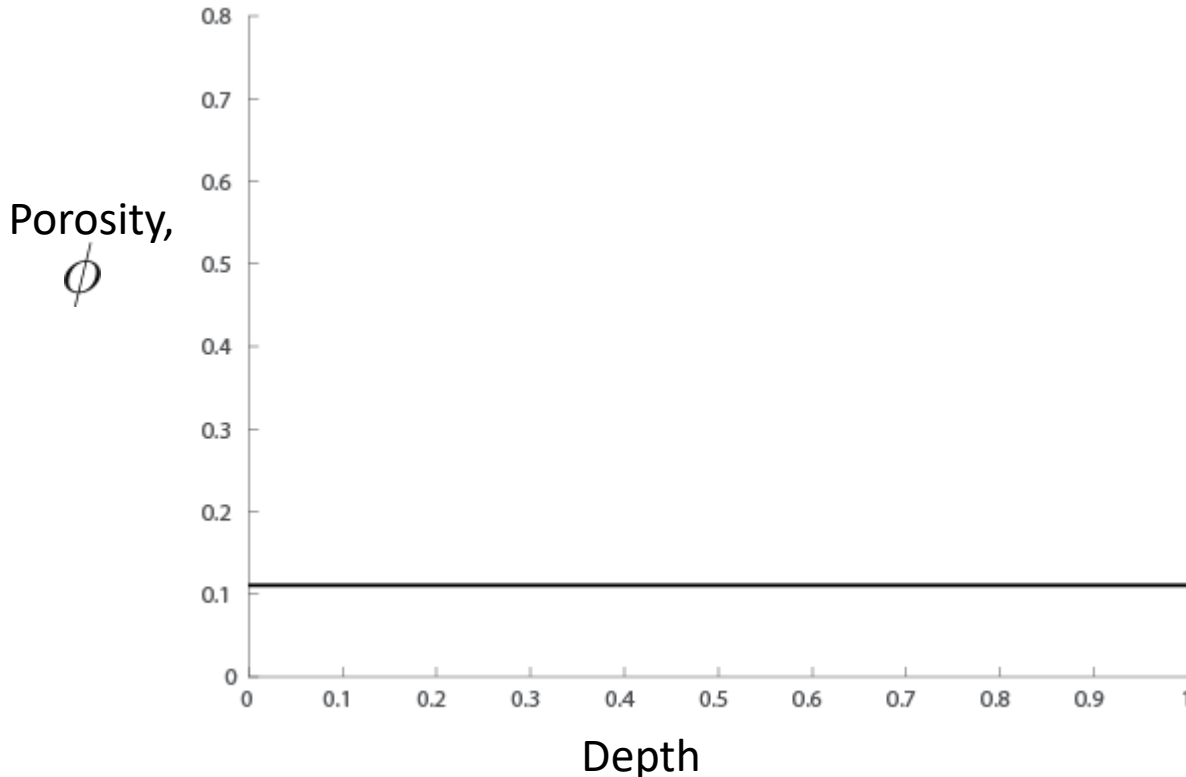
$$\frac{\partial c}{\partial t} = \nabla \left( \tilde{D}(\phi) \nabla c - \mathbf{u}(\phi) c + (\tilde{A}(\phi) \nabla \phi) c \right) - \tilde{k}(\phi)$$

$$\frac{\partial R}{\partial t} = -\beta \frac{\partial c(R, t)}{\partial r}$$

$$t = \tau/\beta$$
$$\beta \ll 1$$

# The filter that traps the most contaminant

- A filter that traps the most contaminant will **block everywhere at once**.



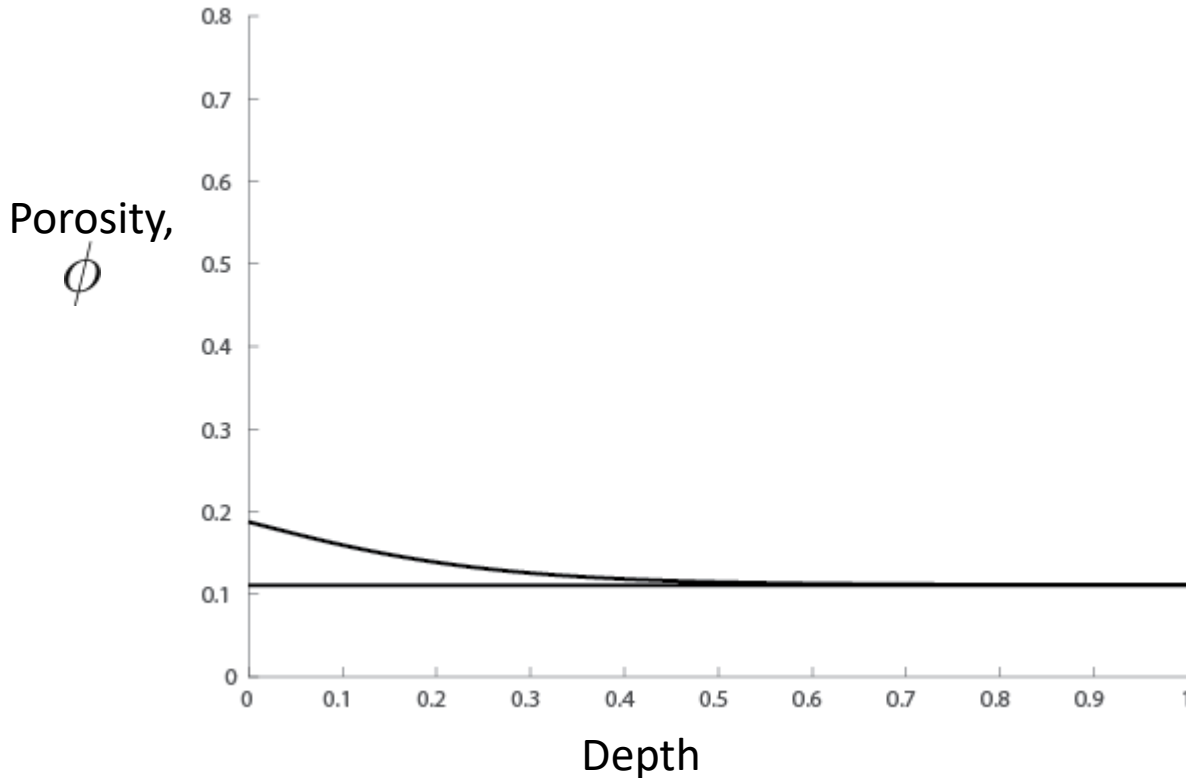
$$\cancel{\frac{\partial c}{\partial t}} = \nabla \left( \tilde{D}(\phi) \nabla c - \mathbf{u}(\phi) c + (\tilde{A}(\phi) \nabla \phi) c \right) - \tilde{k}(\phi)$$

$$\frac{\partial R}{\partial \tau} = -\frac{\partial c(R, t)}{\partial r}$$

$$t = \tau/\beta$$
$$\beta \ll 1$$

# The filter that traps the most contaminant

- A filter that traps the most contaminant will **block everywhere at once**.



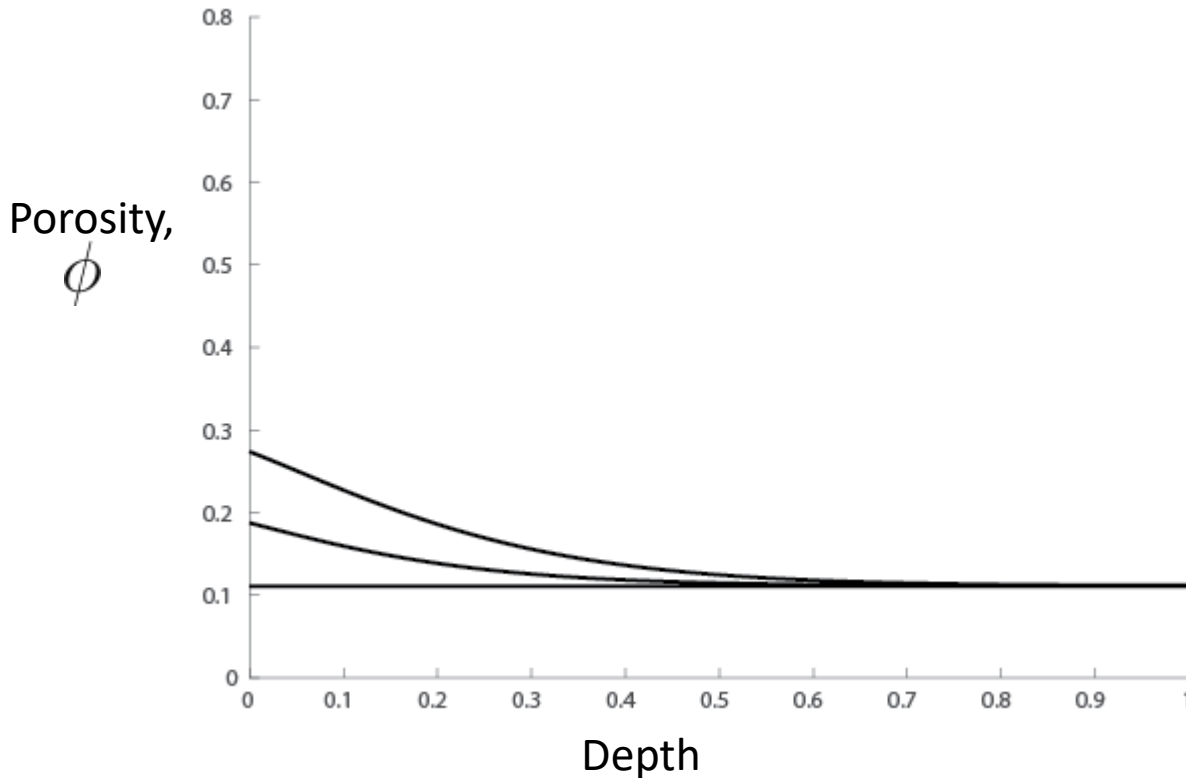
$$\cancel{\frac{\partial c}{\partial t}} = \nabla \left( \tilde{D}(\phi) \nabla c - \mathbf{u}(\phi) c + (\tilde{A}(\phi) \nabla \phi) c \right) - \tilde{k}(\phi)$$

$$\frac{\partial R}{\partial \tau} = -\frac{\partial c(R, t)}{\partial r}$$

$$t = \tau/\beta$$
$$\beta \ll 1$$

# The filter that traps the most contaminant

- A filter that traps the most contaminant will **block everywhere at once**.



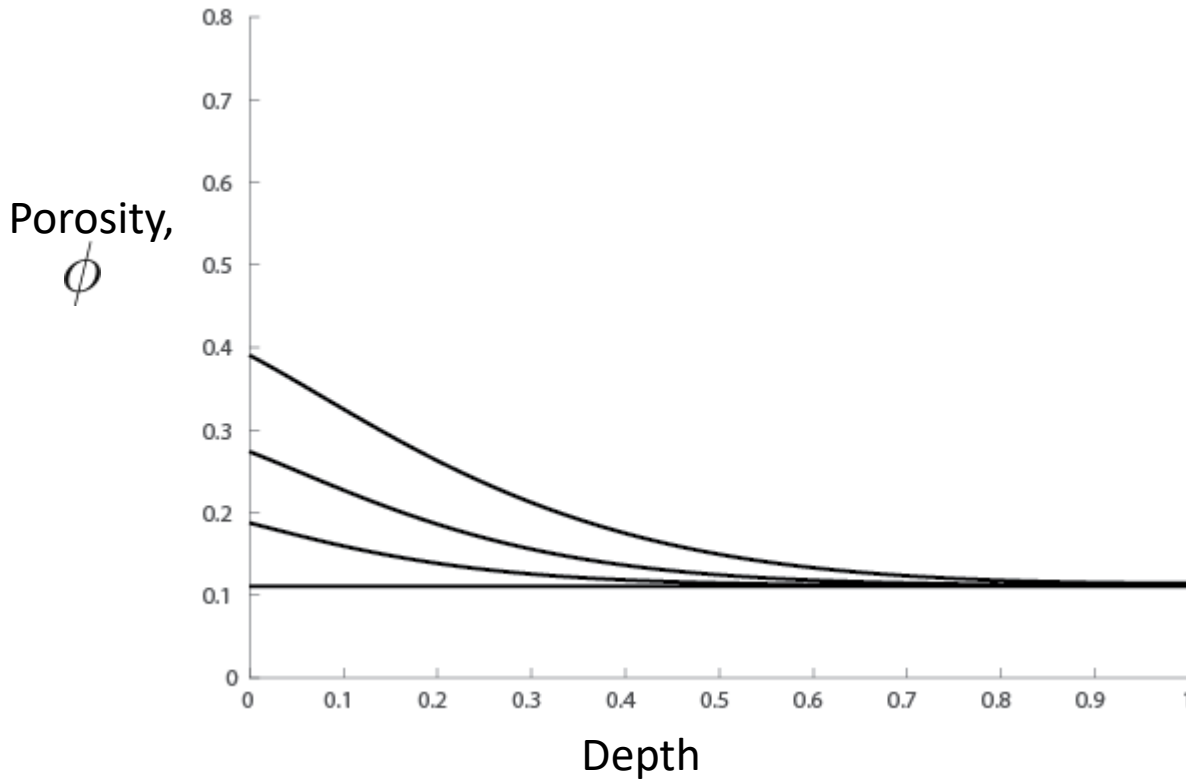
$$\cancel{\frac{\partial c}{\partial t}} = \nabla \left( \tilde{D}(\phi) \nabla c - \mathbf{u}(\phi) c + (\tilde{A}(\phi) \nabla \phi) c \right) - \tilde{k}(\phi)$$

$$\frac{\partial R}{\partial \tau} = -\frac{\partial c(R, t)}{\partial r}$$

$$t = \tau/\beta$$
$$\beta \ll 1$$

# The filter that traps the most contaminant

- A filter that traps the most contaminant will **block everywhere at once**.



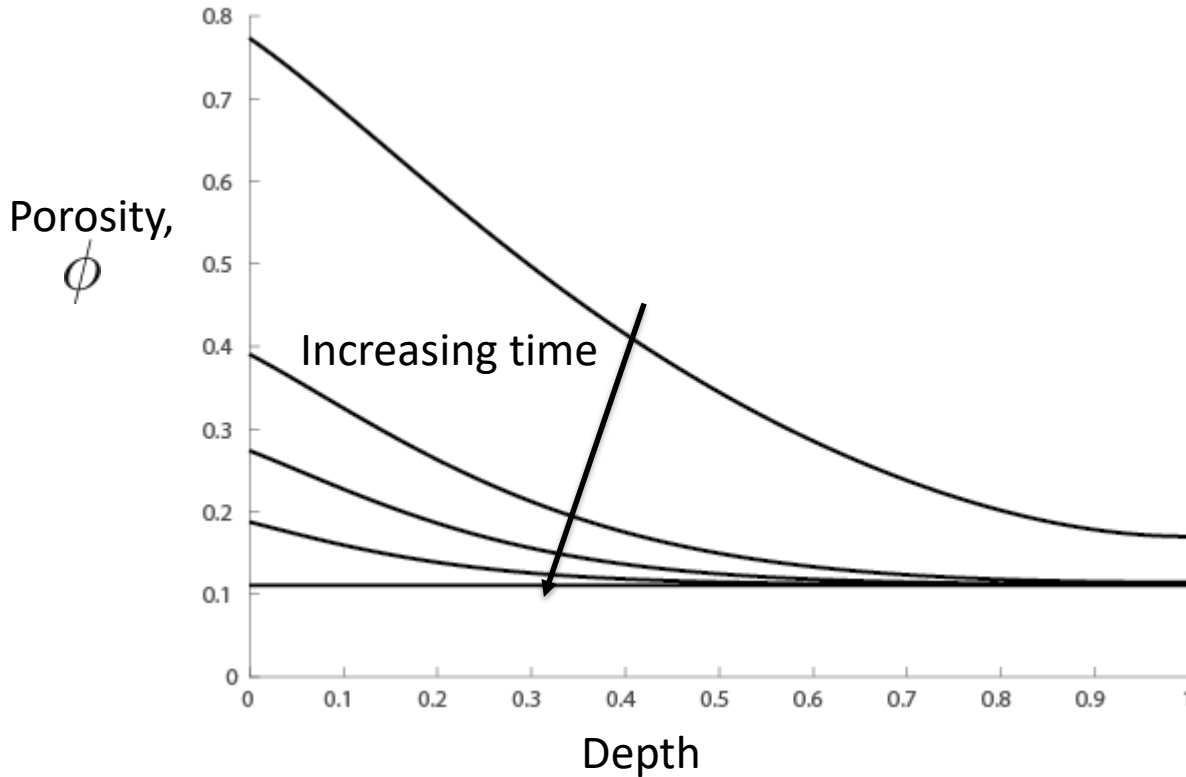
$$\cancel{\frac{\partial c}{\partial t}} = \nabla \left( \tilde{D}(\phi) \nabla c - \mathbf{u}(\phi) c + (\tilde{A}(\phi) \nabla \phi) c \right) - \tilde{k}(\phi)$$

$$\frac{\partial R}{\partial \tau} = -\frac{\partial c(R, t)}{\partial r}$$

$$t = \tau/\beta$$
$$\beta \ll 1$$

# The filter that traps the most contaminant

- A filter that traps the most contaminant will **block everywhere at once**.



$$\cancel{\frac{\partial c}{\partial t}} = \nabla \left( \tilde{D}(\phi) \nabla c - \mathbf{u}(\phi) c + (\tilde{A}(\phi) \nabla \phi) c \right) - \tilde{k}(\phi)$$

$$\frac{\partial R}{\partial \tau} = -\frac{\partial c(R, t)}{\partial r}$$

$$t = \tau/\beta$$
$$\beta \ll 1$$

# *State of play*

- Our models are useful in a range of different filtration industries:



**dyson**



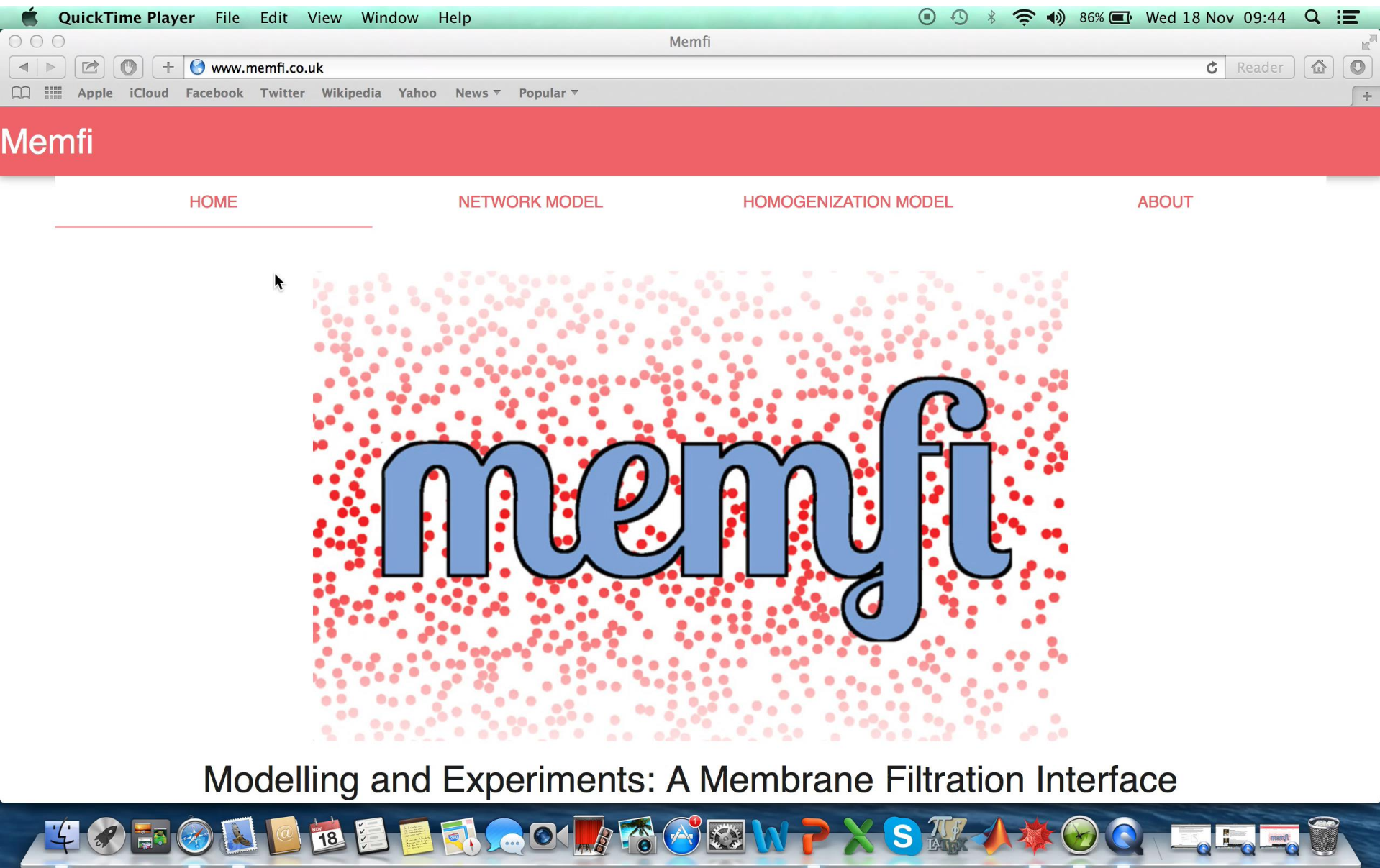
UK Government  
Decontamination  
Service



# *Conveying these results to industry*

- Having obtained a model that allows filtration scientists to understand and interpret the results of their data we provide an online platform that facilitates user interaction [www.memfi.co.uk](http://www.memfi.co.uk)

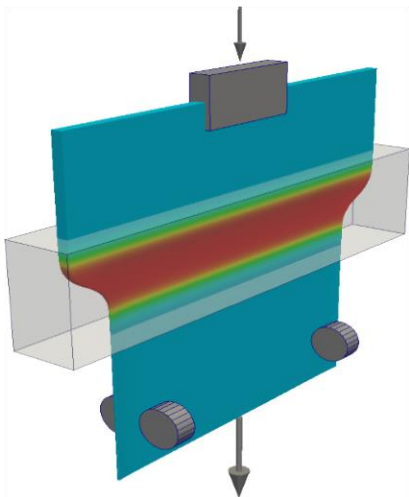
The screenshot shows a web browser window with the title bar "Memfi" and the URL "www.memfi.co.uk". The page has a red header with the word "Memfi" in white. Below the header is a navigation menu with four items: "HOME" (underlined), "NETWORK MODEL", "HOMOGENIZATION MODEL", and "ABOUT". The main content area features a large blue "memfi" logo centered over a background of red and pink circular dots. Below the logo, the text "Modelling and Experiments: A Membrane Filtration Interface" is displayed. At the bottom left is the University of Oxford logo, and at the bottom right is the text "Mathematical Institute", "DEPARTMENT OF COMPUTER SCIENCE", and "(C) 2015. Dr. Ian Griffiths, Dr. Maria Bruna, Dr. Mohit Dalwadi".



# *Glass sheet manufacture*

SCHOTT

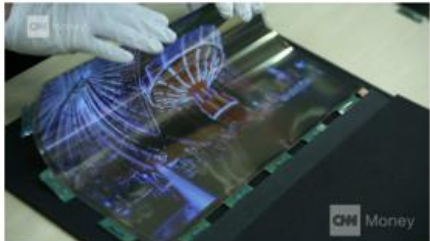
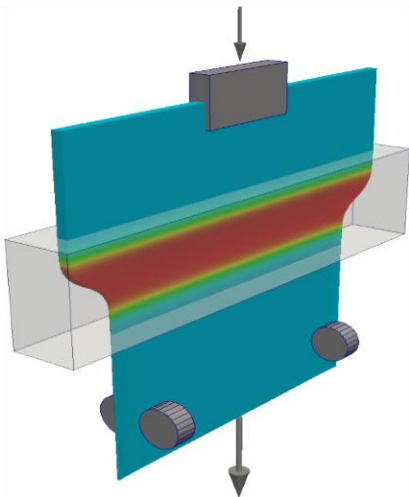
- How do we make the thin glass sheets for mobile phones?
- We use the **redraw process** where a glass block is fed into a heater zone and stretched outwards.



# Glass sheet manufacture

SCHOTT

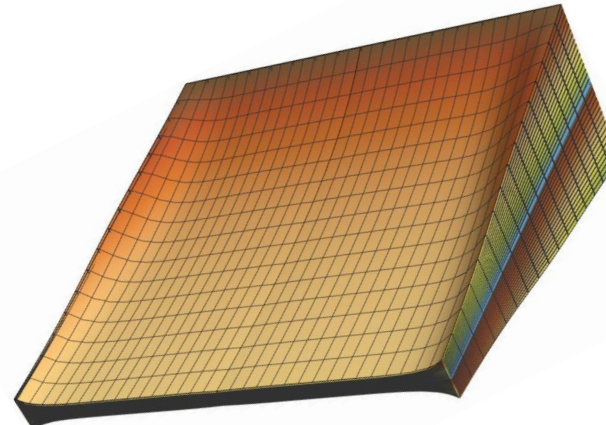
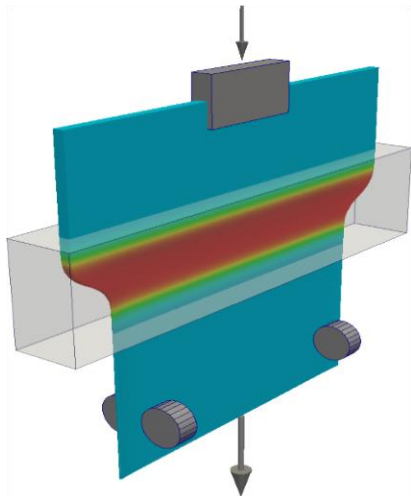
- How do we make the thin glass sheets for mobile phones?
- We use the **redraw process** where a glass block is fed into a heater zone and stretched outwards.



- The glass is also used for flexible devices.

# *Glass sheet manufacture*

- As the glass is stretched down it **gathers in** from the edges, resulting in **thicker glass at the edges**:



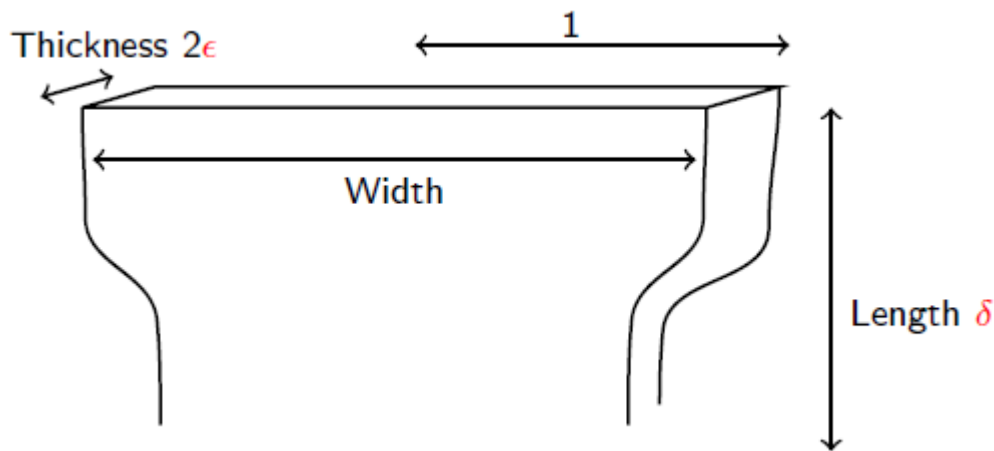
- This makes transportation difficult.
- How can we avoid the thick edges?



# *A mathematical model*

We consider

- A **steady-state process**, where the glass sheet has a **prescribed temperature** (and viscosity) profile that varies with longitudinal position  $x$ .
- **Three-dimensional Stokes flow**.
- **No surface tension**.
- Sheet thickness  $\ll$  heater zone length  $\ll$  sheet width.



$$\epsilon \ll \delta \ll 1$$

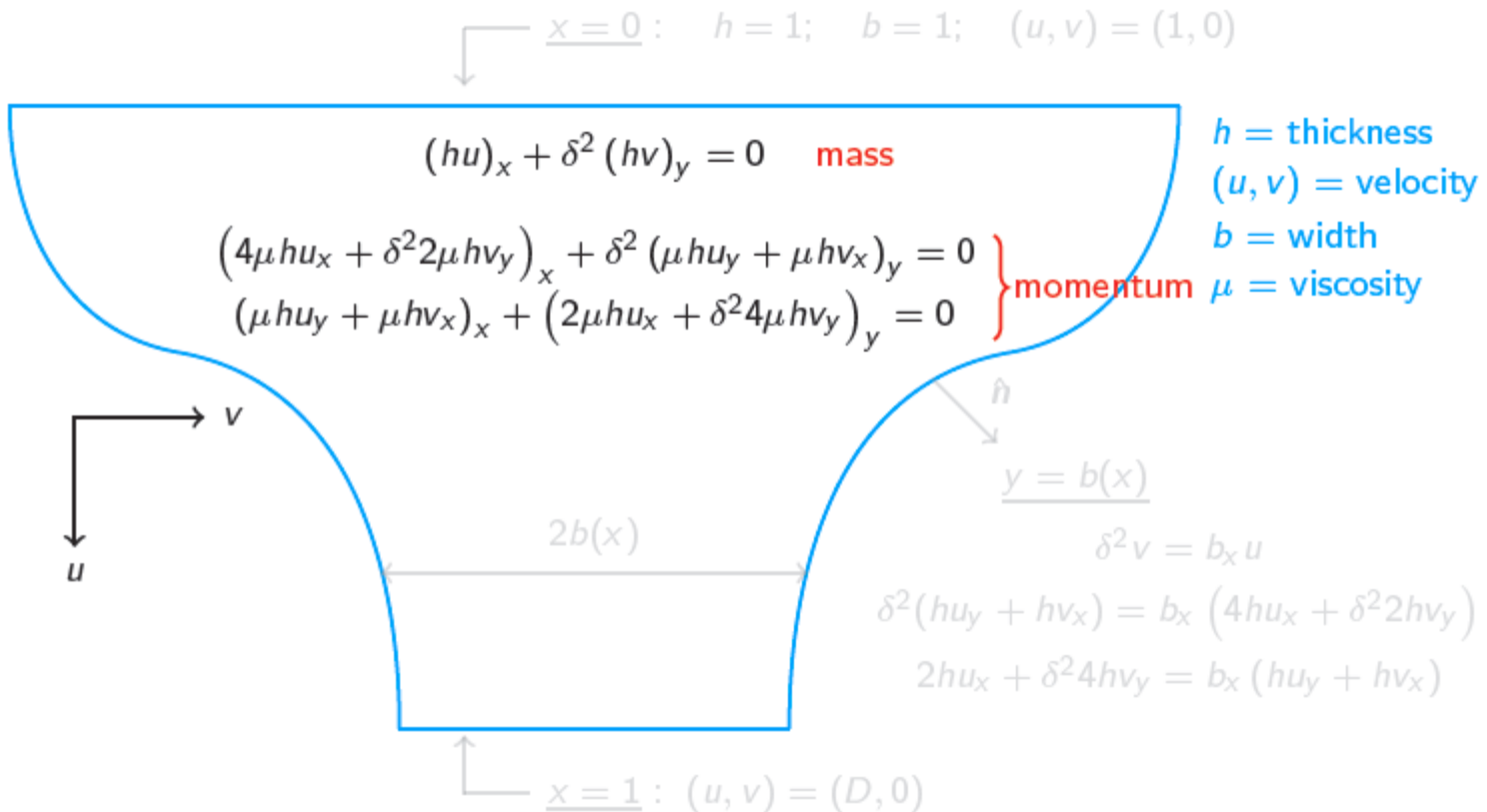
$\epsilon$  = preform thickness/  
preform width

$\delta$  = heater zone length/  
preform half-width

# Model reduction

- Exploiting  $\epsilon \ll 1$  reduces the problem to two dimensions:

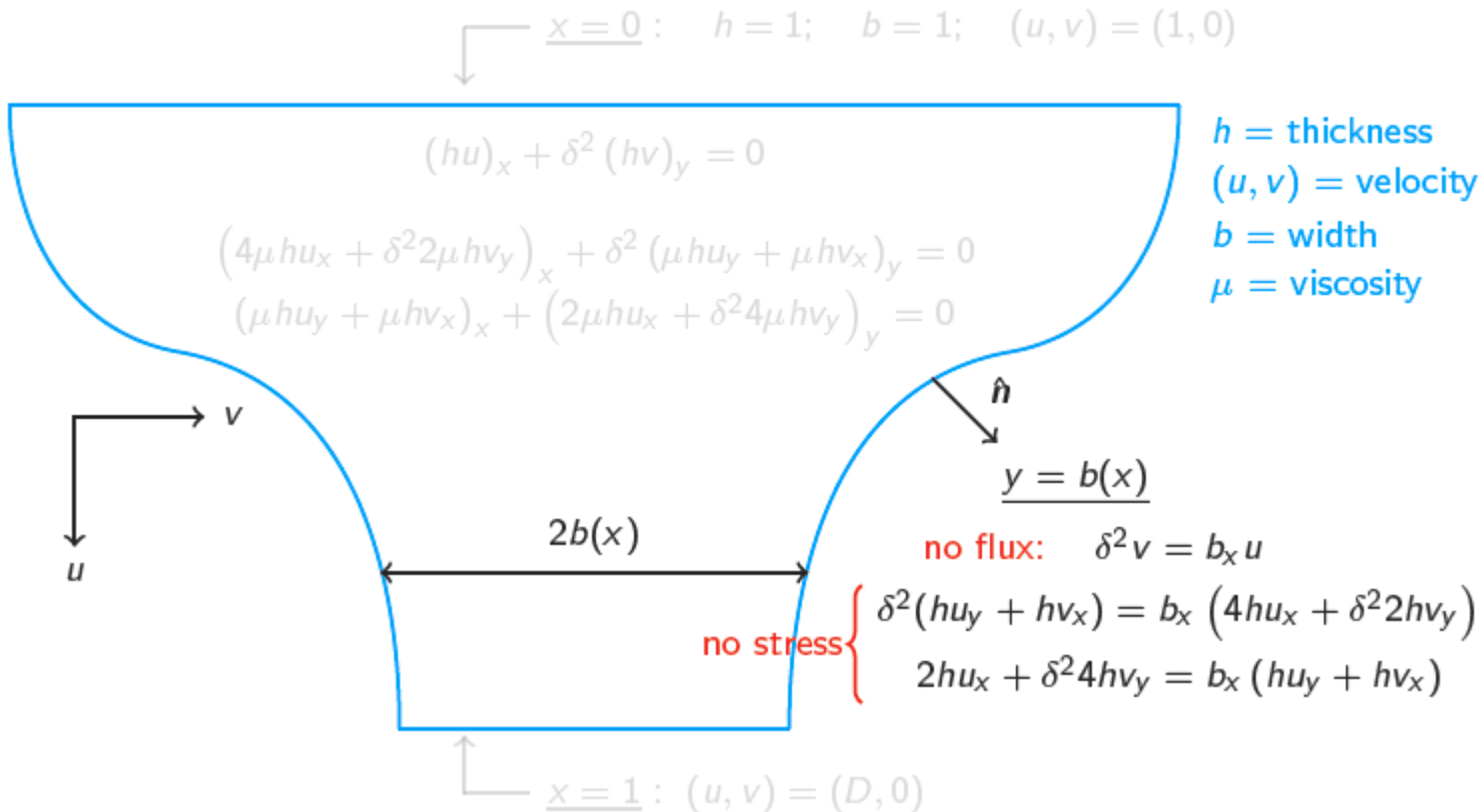
$\epsilon \ll \delta \ll 1$   
 $\epsilon = \text{preform thickness/width}$   
 $\delta = \text{length/half-width}$



# Model reduction

- Exploiting  $\epsilon \ll 1$  reduces the problem to two dimensions:

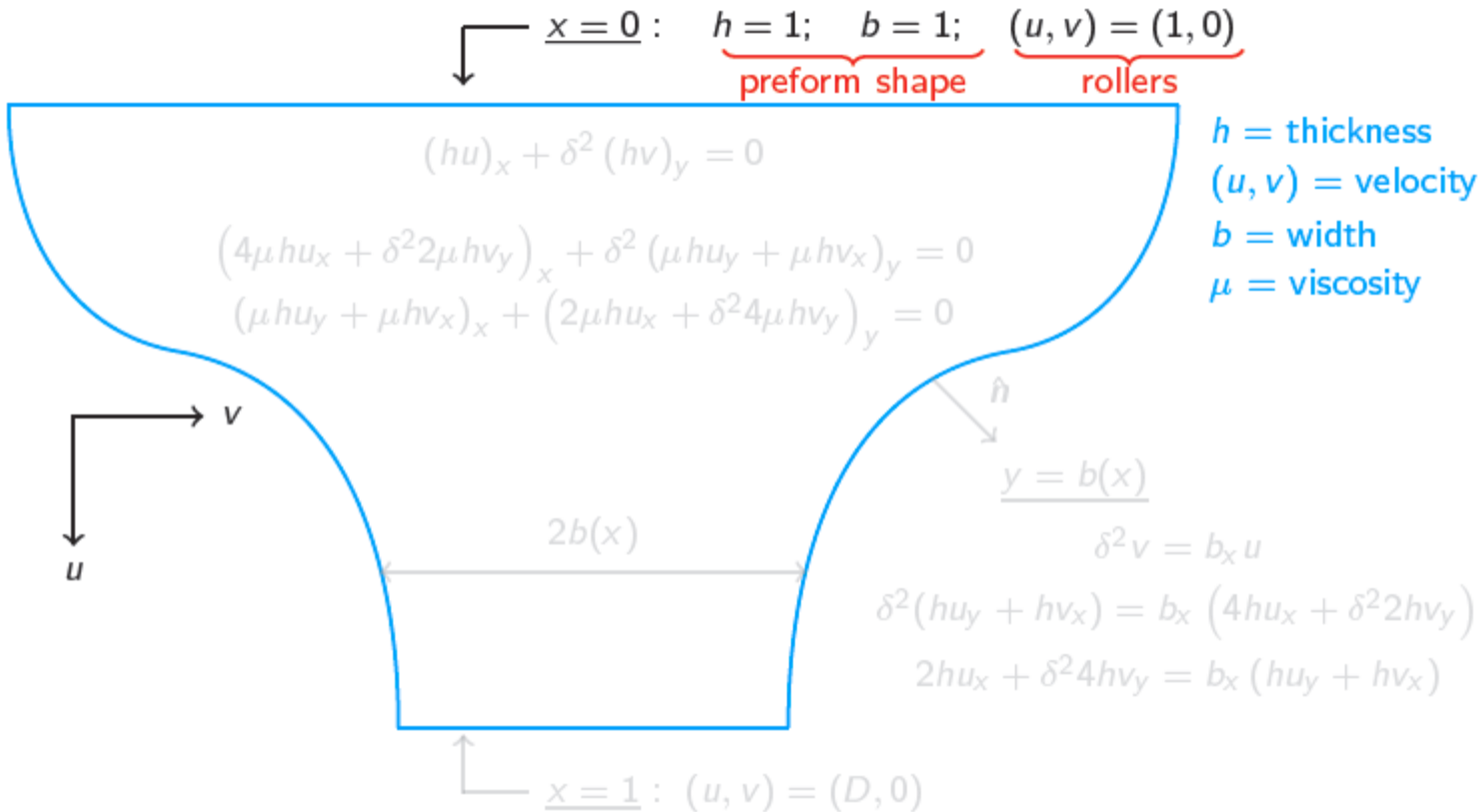
$\epsilon \ll \delta \ll 1$   
 $\epsilon = \text{preform thickness/width}$   
 $\delta = \text{length/half-width}$



# Model reduction

- Exploiting  $\epsilon \ll 1$  reduces the problem to two dimensions:

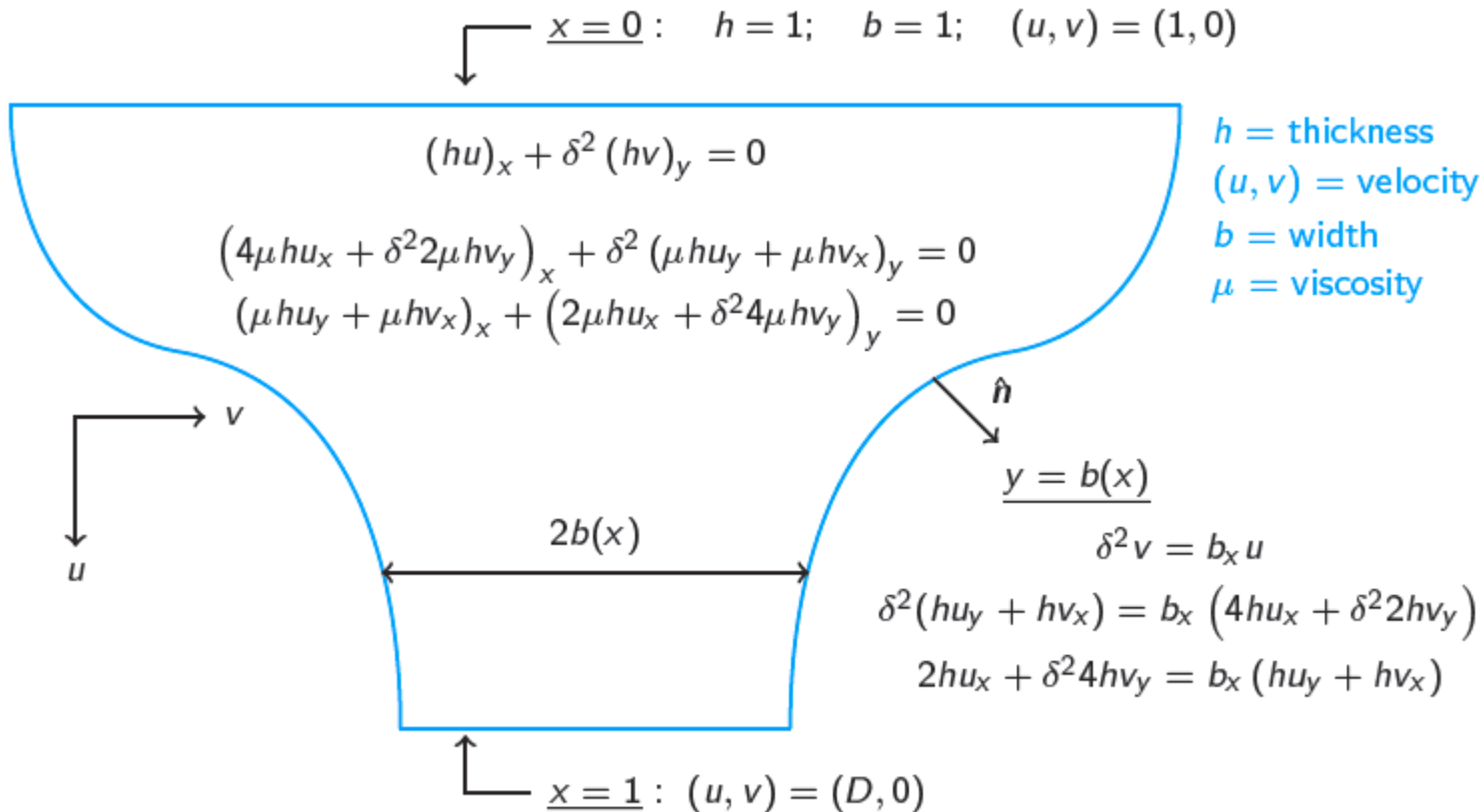
$\epsilon \ll \delta \ll 1$   
 $\epsilon = \text{preform thickness/width}$   
 $\delta = \text{length/half-width}$



# Model reduction

- Exploiting  $\epsilon \ll 1$  reduces the problem to two dimensions:

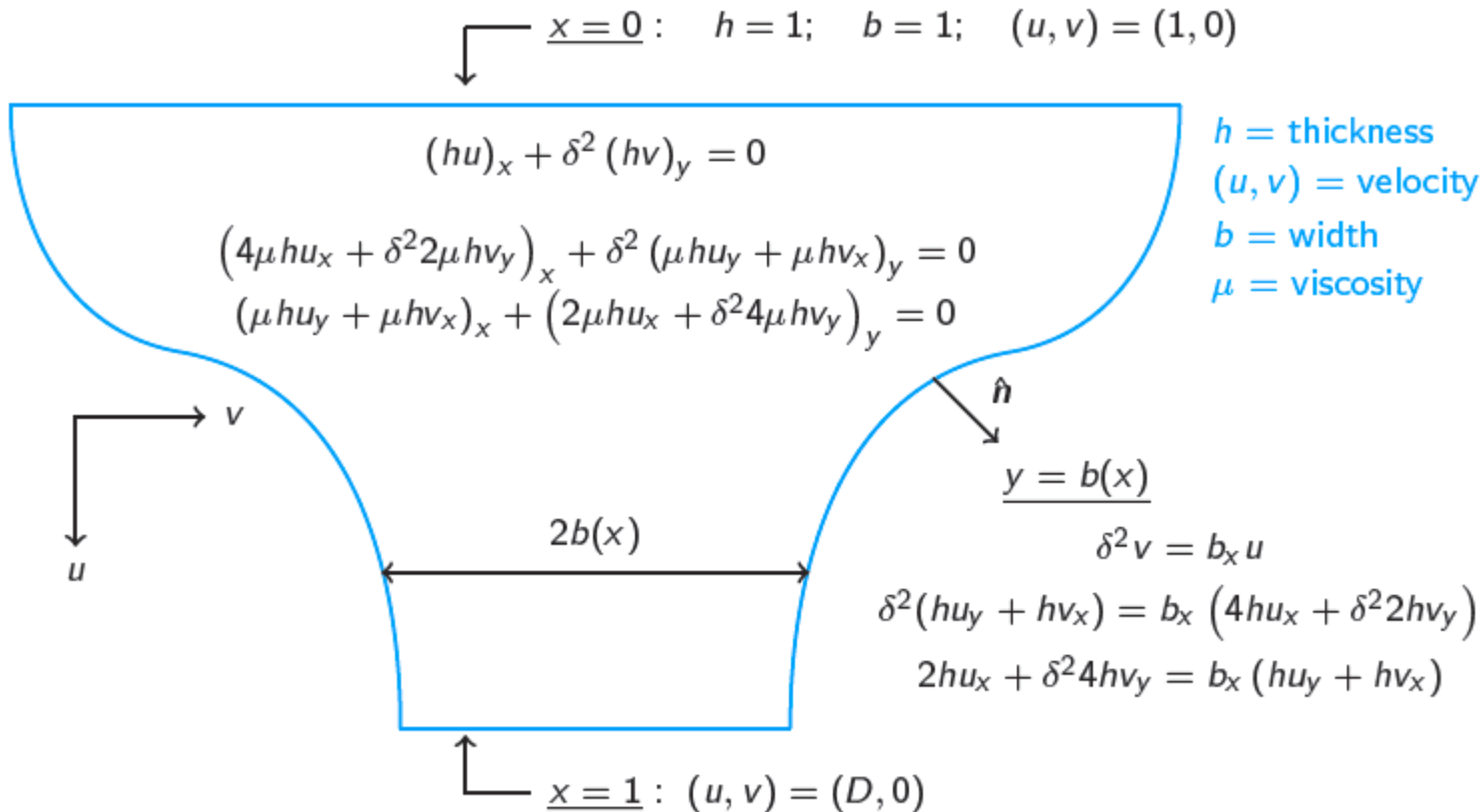
$\epsilon \ll \delta \ll 1$   
 $\epsilon = \text{preform thickness/width}$   
 $\delta = \text{length/half-width}$



# Model reduction

- Exploiting  $\epsilon \ll 1$  reduces the problem to two dimensions:

$\epsilon \ll \delta \ll 1$   
 $\epsilon = \text{preform thickness/width}$   
 $\delta = \text{length/half-width}$



What about  $\delta \rightarrow 0$ ?

# Model reduction

$$\varepsilon \ll \delta \ll 1$$

$\varepsilon$  = preform thickness/width

$\delta$  = length/half-width

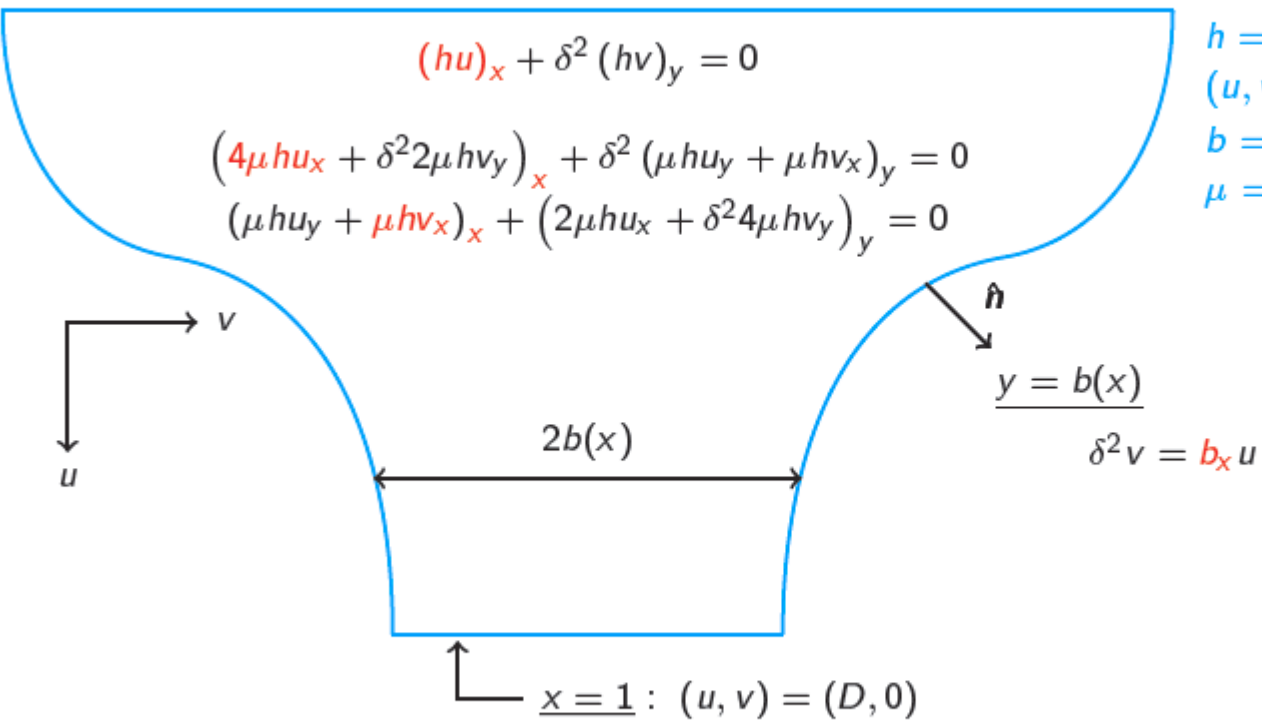
$\xrightarrow{x=0} : h = 1; b = 1; (u, v) = (1, 0)$

$$(hu)_x + \delta^2 (hv)_y = 0$$

$$(4\mu hu_x + \delta^2 2\mu hv_y)_x + \delta^2 (\mu hu_y + \mu hv_x)_y = 0$$

$$(\mu hu_y + \mu hv_x)_x + (2\mu hu_x + \delta^2 4\mu hv_y)_y = 0$$

$h$  = thickness  
 $(u, v)$  = velocity  
 $b$  = width  
 $\mu$  = viscosity



What about  $\delta \rightarrow 0$ ?

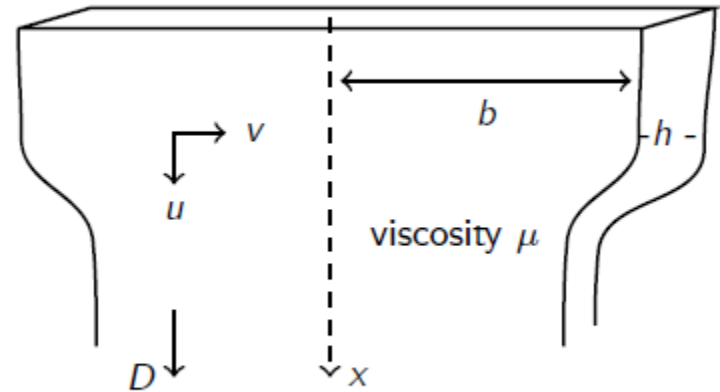
# Model reduction

At leading order in  $\delta$ :

$$u(x) = \exp \left( \ln D \frac{\int_0^x \frac{ds}{\mu(s)}}{\int_0^1 \frac{ds}{\mu(s)}} \right),$$

$$h(x) = \exp \left( -\ln D \frac{\int_0^x \frac{ds}{\mu(s)}}{\int_0^1 \frac{ds}{\mu(s)}} \right),$$

$$v = 0, \quad b = 1.$$



Final thickness  $h(1) = 1/D$ .

Doesn't satisfy edge stress conditions  
⇒ **boundary layer**



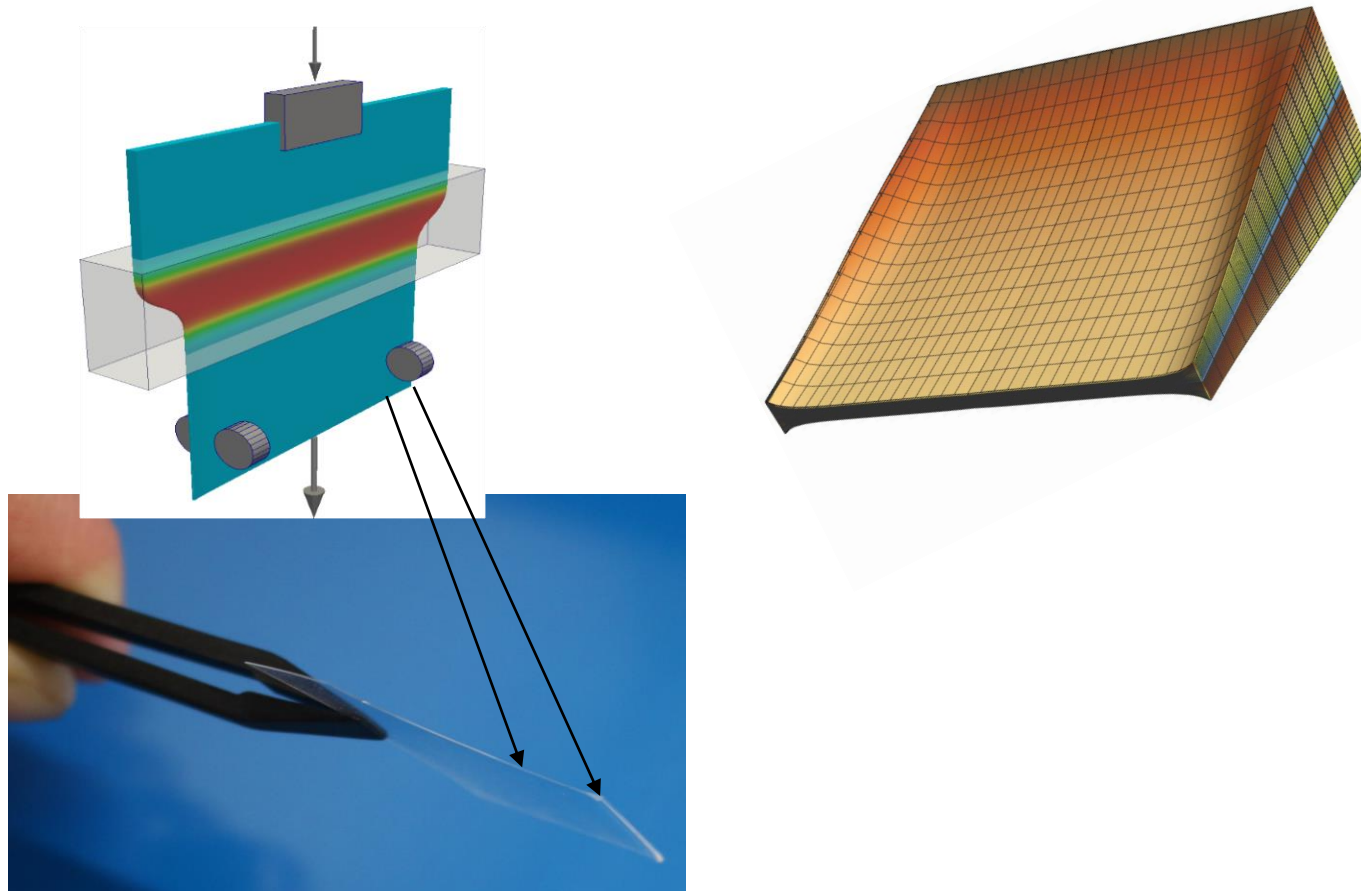
# *Model reduction*

- Scaling into the boundary layer we recover the full two-dimensional equations and free boundary conditions.
- Requires numerical solution, **but** removes  $\delta$  from the problem and now depends only on draw ratio,  $D$ , and viscosity.
- As  $Y \rightarrow -\infty$  match with one-dimensional outer solution.

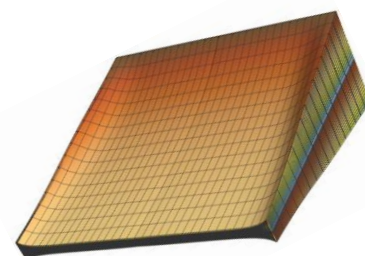
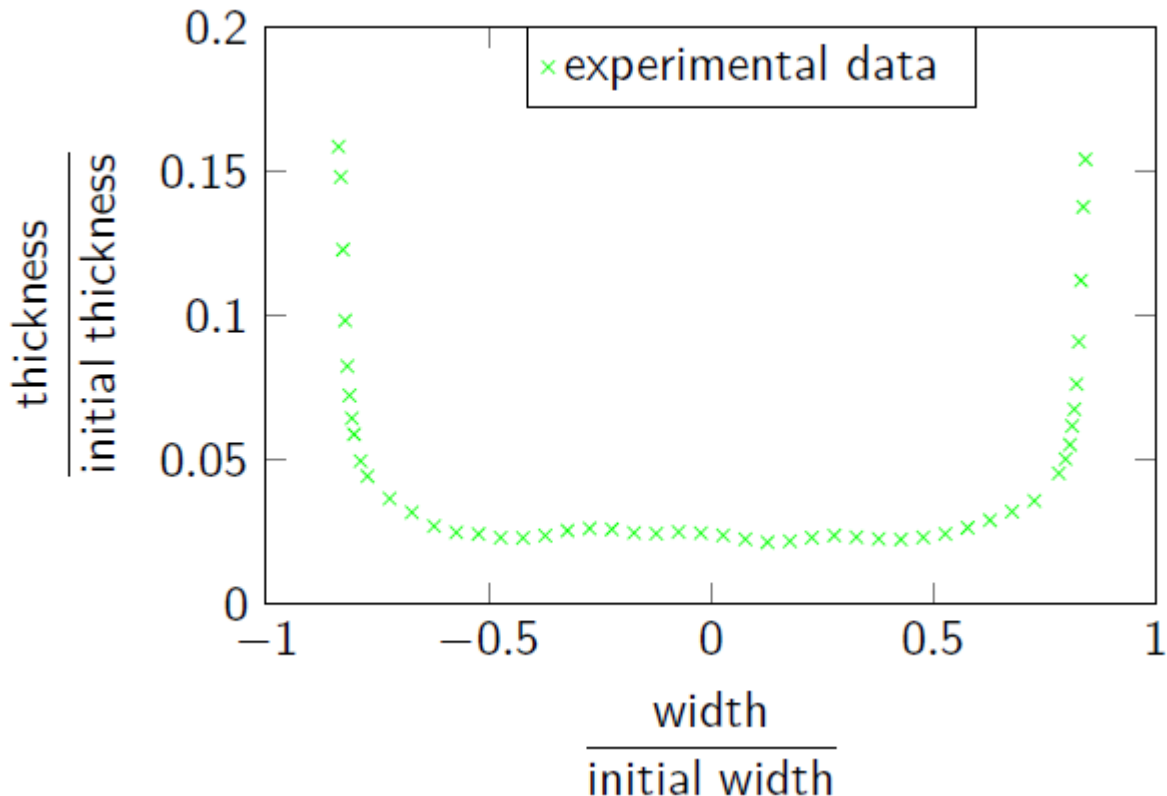


# *Solutions*

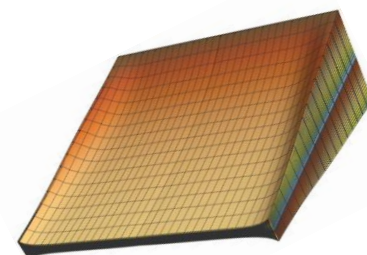
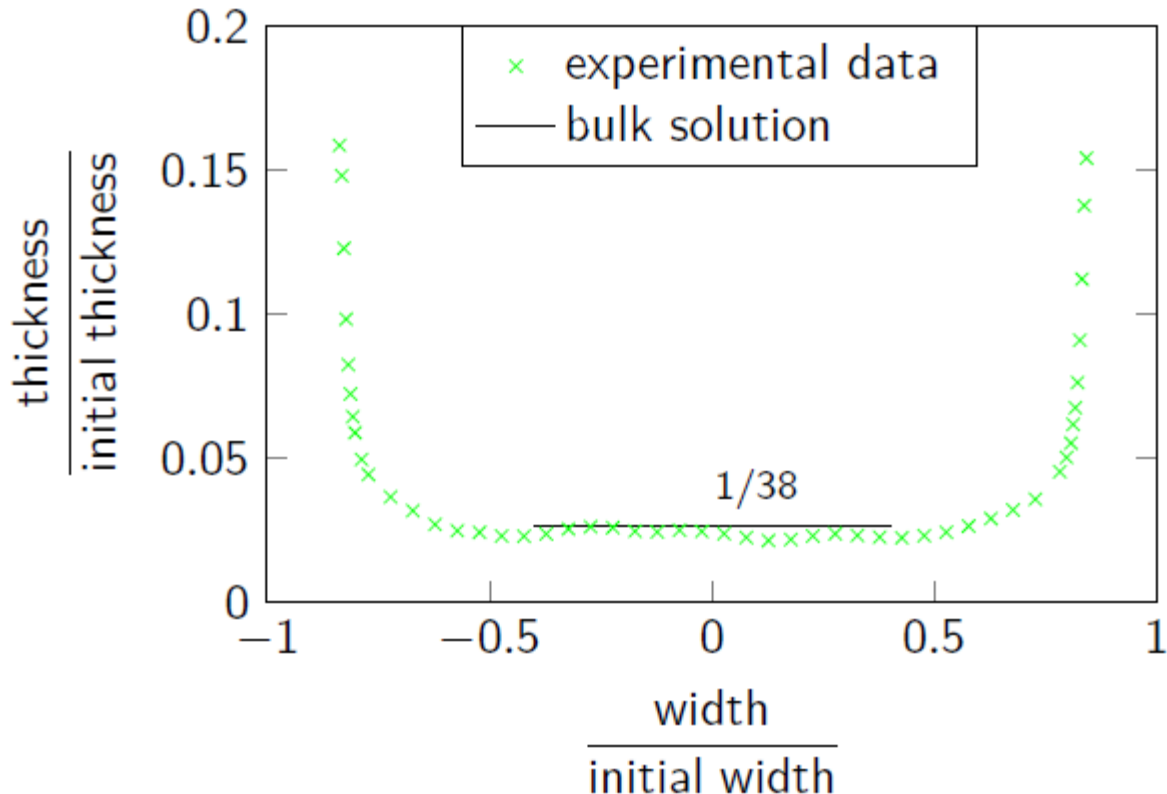
- A rectangular preform draws to a non-rectangular final cross-section.
- Glass is gathered by the inward-moving edge.
- This is exactly what is observed in practice.



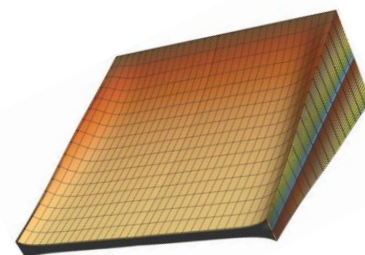
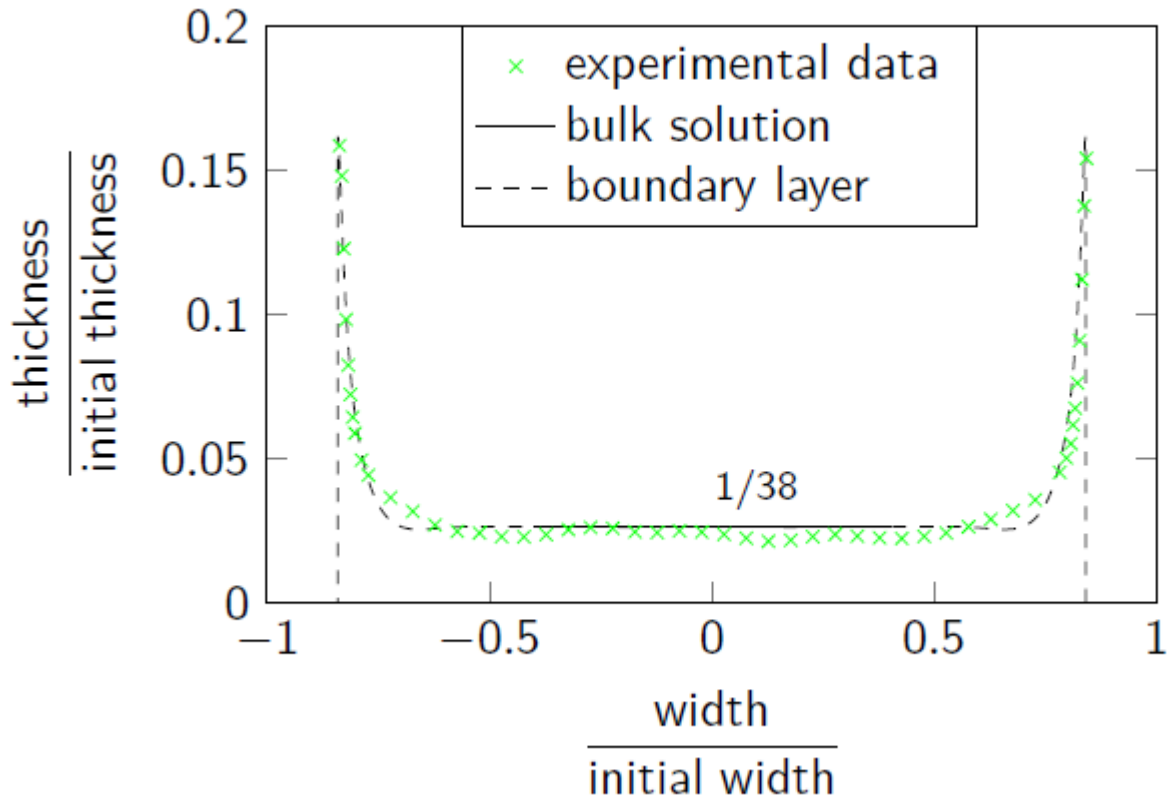
# *Comparison with experiments*



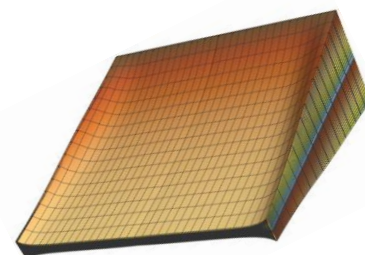
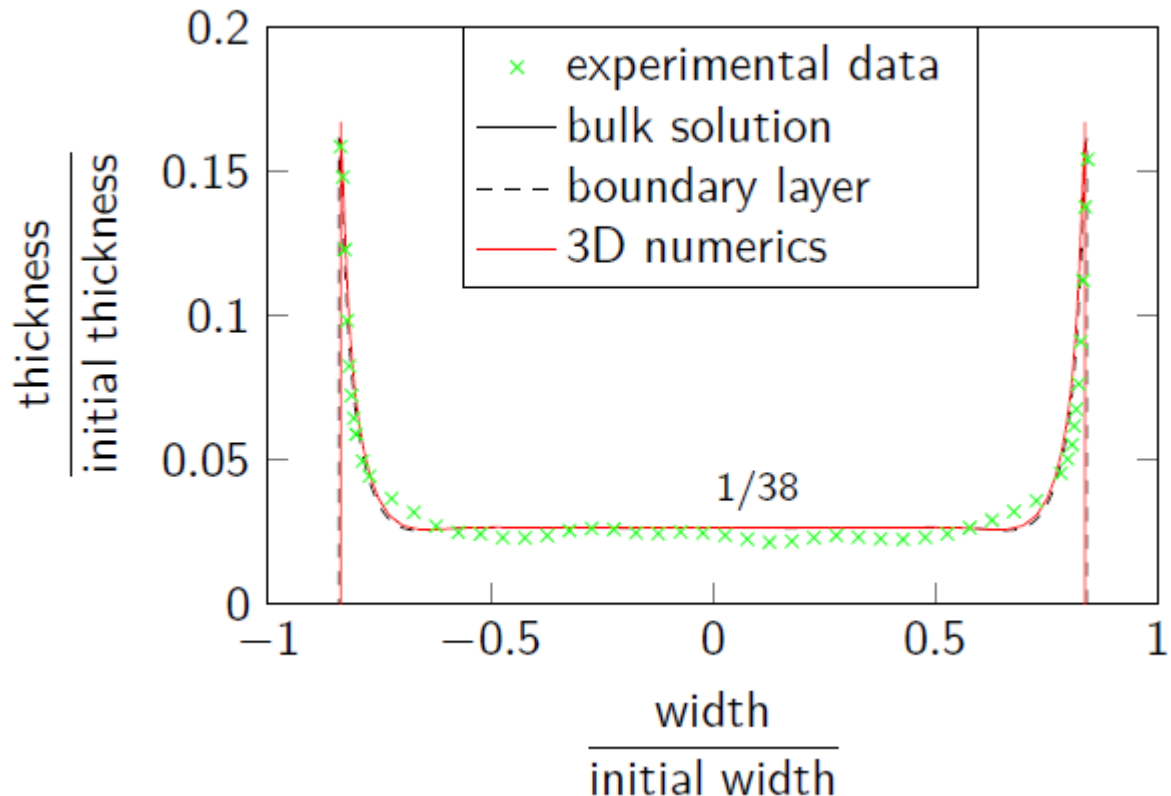
# *Comparison with experiments*



# *Comparison with experiments*

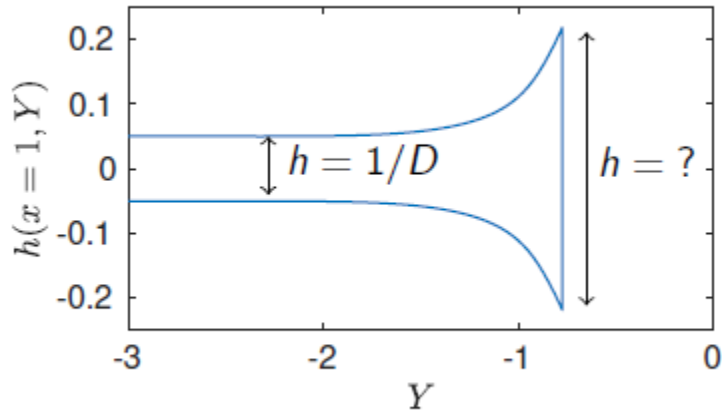


# *Comparison with experiments*



# How do we avoid thick edges?

- The thickness scales with  $1/D$  in the bulk.



- Using curvilinear coordinates at the sheet edge gives:

$$h\sqrt{|\mathbf{u}|} = \text{constant}$$

- So  $h \sim 1/\sqrt{D}$  at the edge

- This means that **edge thickening worsens with increasing draw ratio.**

# *How do we avoid thick edges?*

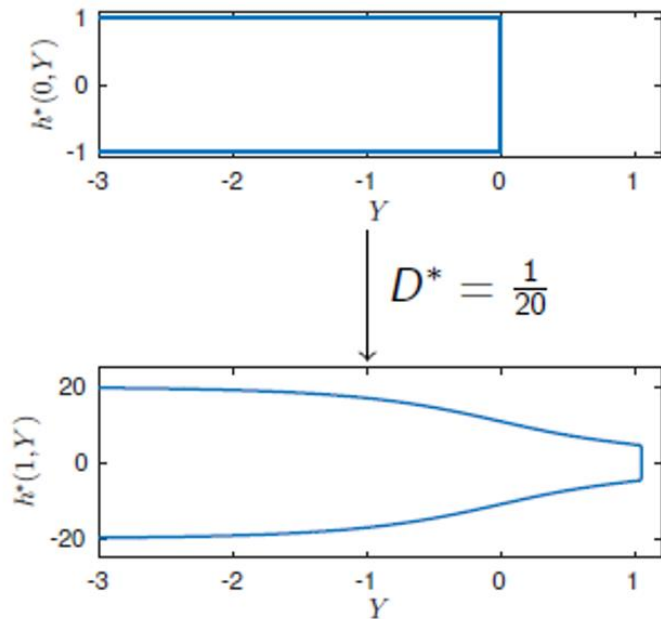
- Can we make a rectangular product by using a preform with an appropriate shape?



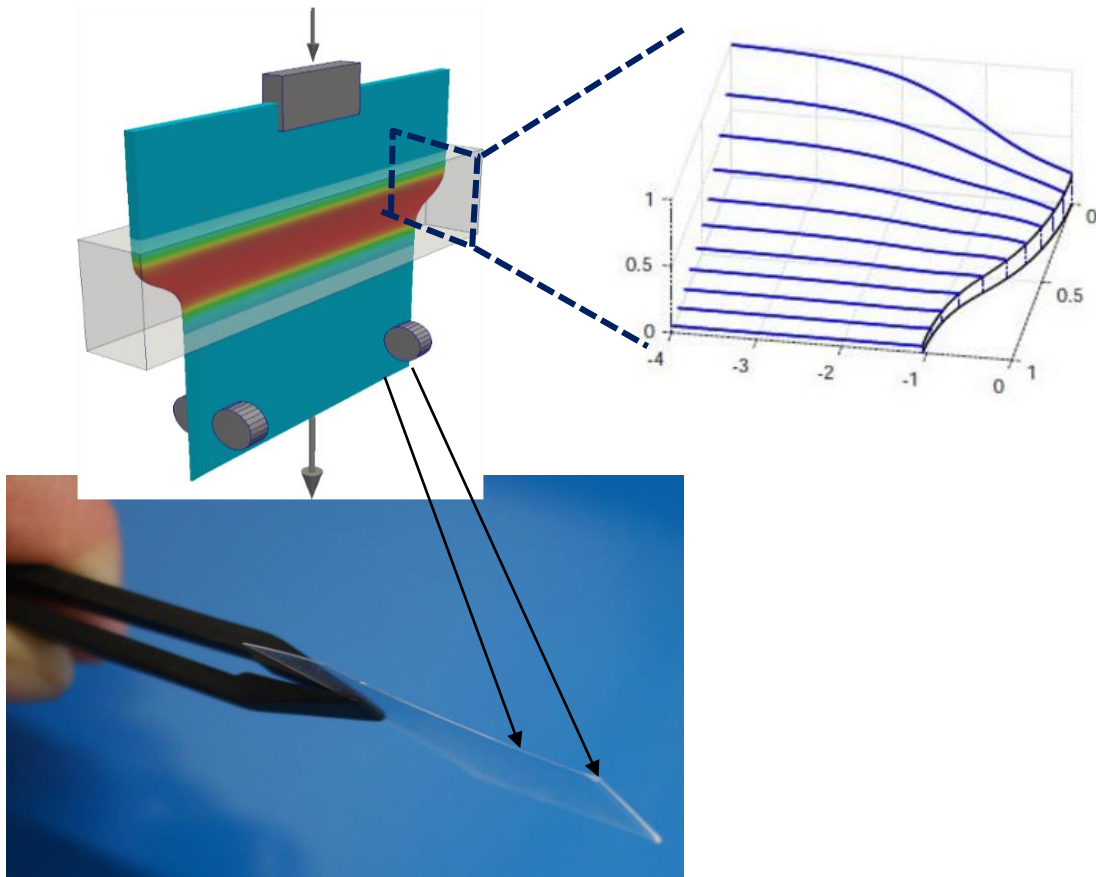
- This is an **inverse problem**: given the final shape what should the initial shape be?
- We can exploit symmetry to turn this into a version of the forward problem.

# How do we avoid thick edges?

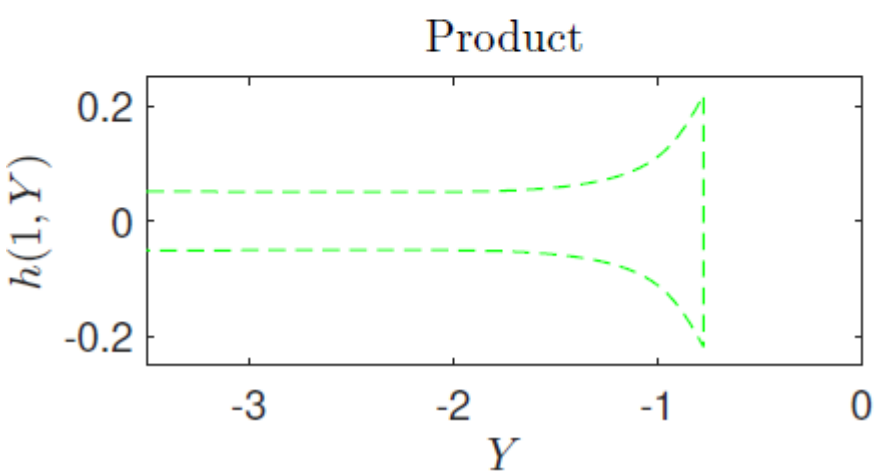
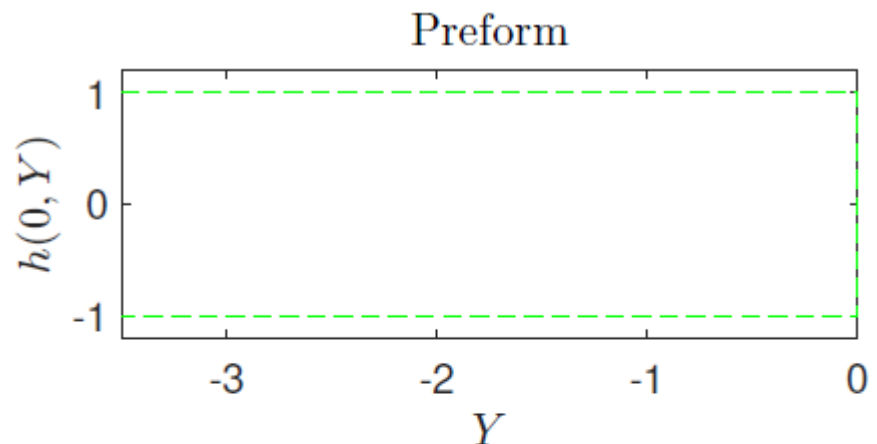
- Solve forward problem with draw ratio  $D^* = 1/D < 1$ .
- Read off resulting thickness profile  $h^*(1, Y)$ .
- Required preform shape is  $h(0, Y) = 1/D h^*(1, Y)$ .



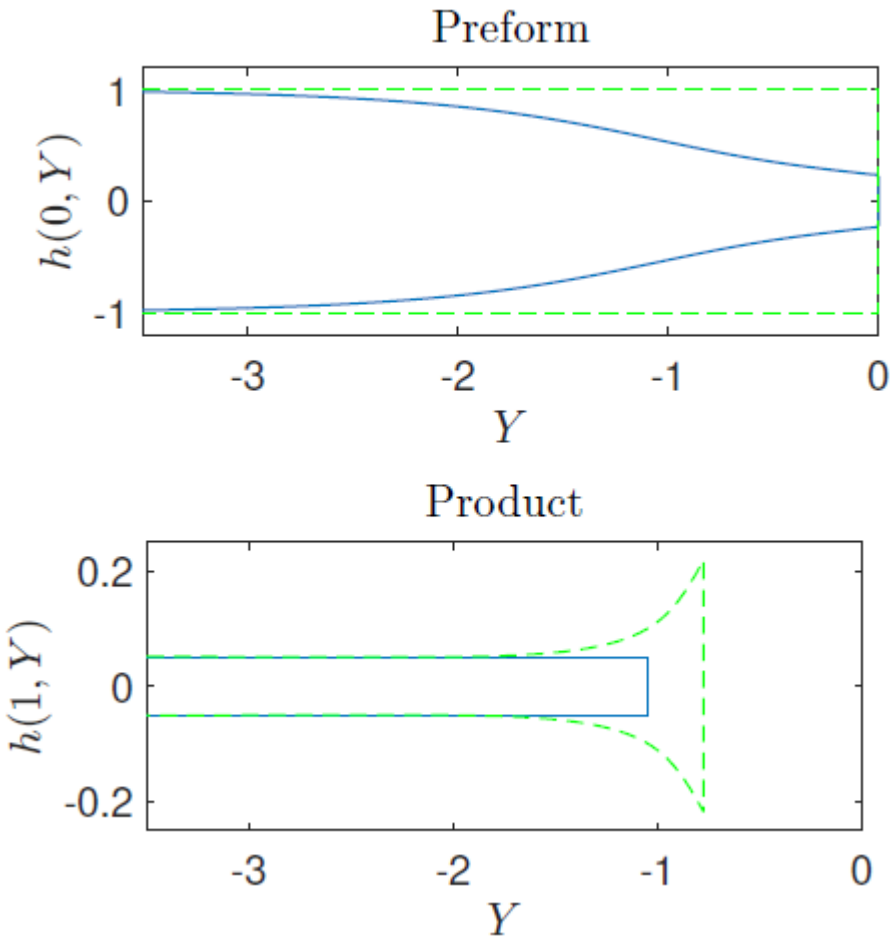
# *An optimal preform*



# *Making uniformly thick glass*

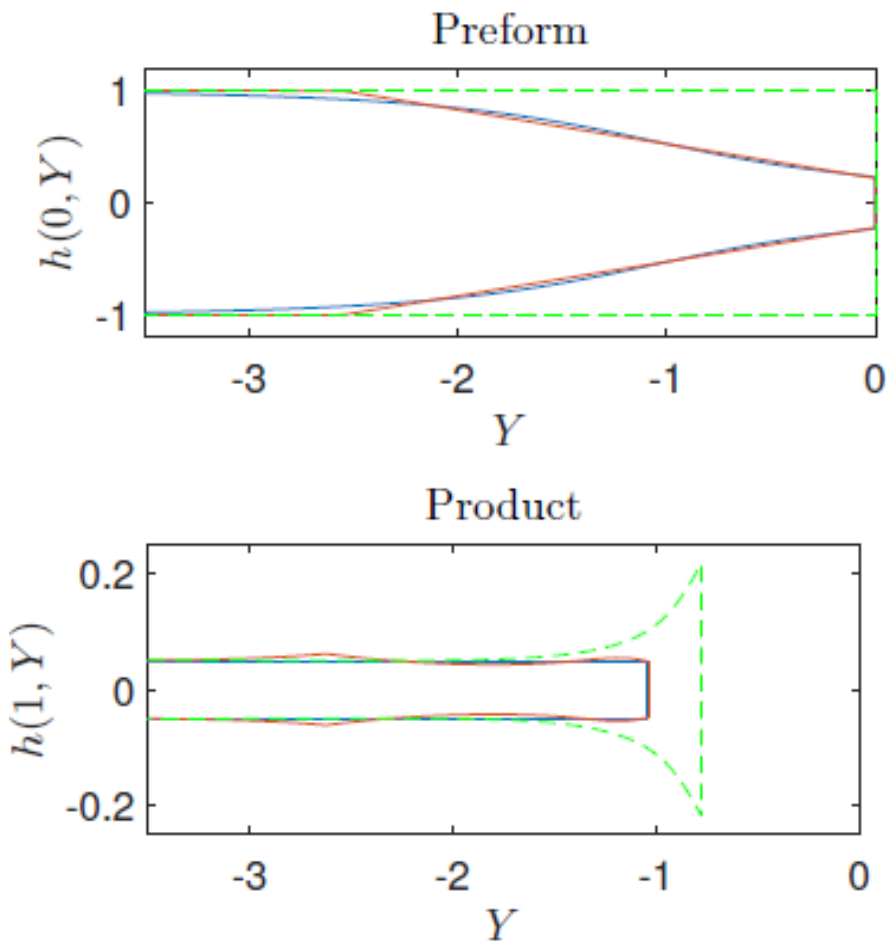


# *Making uniformly thick glass*



- In practice there are limitations on the preform shape.
- But we can do a linear taper instead.
- A sharp corner in the preform leads to a kink in the final product.

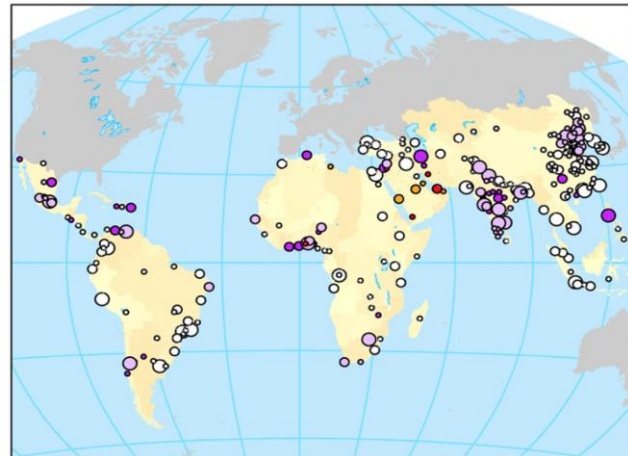
# *Making uniformly thick glass*



- In practice there are limitations on the preform shape.
- But we can do a linear taper instead.
- A sharp corner in the preform leads to a kink in the final product.

# *Closing thoughts*

Filter lifetime

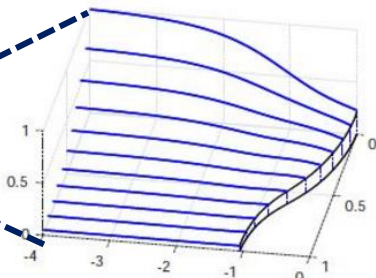
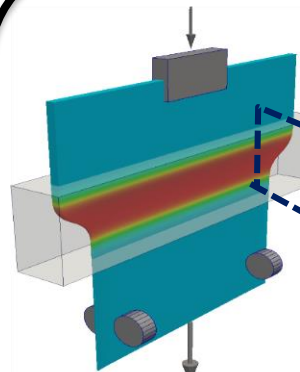
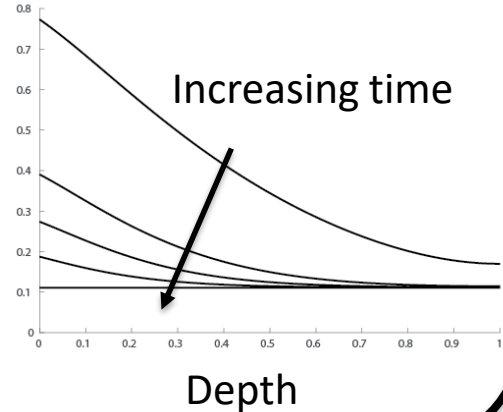


dyson



Porosity

Increasing time



SCHOTT

GM Money

## Network Model

Membrane fouling during particle filtration occurs through a variety of mechanisms, including internal pore clogging by contaminants, coverage of pore entrances, and deposition on the membrane surface. Each of these fouling mechanisms results in a decline in the observed flow rate over time, and the decrease in filtration efficiency can be characterized by a unique signature formed by plotting the volumetric flux,  $Q$ , as a function of the total volume of fluid processed,  $V$ .

When membrane fouling takes place via any one of these mechanisms independently the QV signature is always convex downwards for filtration under a constant transmembrane pressure. However, in many such filtration scenarios, the fouling mechanisms are inherently coupled and the resulting signature is more difficult to interpret. For instance, blocking of a pore entrance will be exacerbated by the internal clogging of a pore, while the deposition of a layer of contaminants is more likely once the pores have been covered by particulates. As a result, the experimentally observed QV signature can vary dramatically from the canonical convex downwards graph, revealing features that are not captured by existing continuum models. In a range of industrially relevant cases we observe a *concave-downwards* QV signature, indicative of a fouling rate that becomes more severe with time.

This network model allows the user to explore the inter-relation between fouling mechanisms to demonstrate the impact on the QV signature.

[link to this](#)

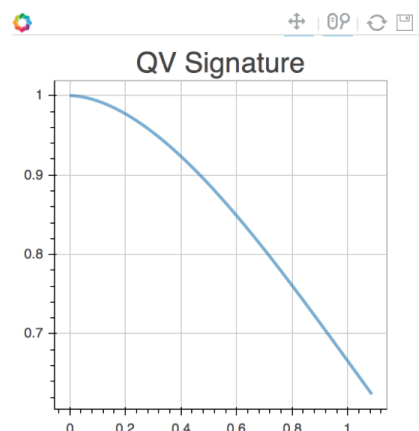
Concentration of Solution ( $c$ ): **0.604**

Adhesivity ( $k$ ): **1**

Leakage Flux ( $Q^*$ ): **0.109**

Flux at total throughput ( $Q_{min}$ ): **0.6238**

show experimental data  
 hide



## Publication

[A combined network model for membrane fouling](#), 2014, I.M. Griffiths, A. Kumar & P.S. Stewart. *J. Coll. Interf. Sci.* 432, 10.

## Network Model

Membrane fouling during particle filtration occurs through a variety of mechanisms, including internal pore clogging by contaminants, coverage of pore entrances, and deposition on the membrane surface. Each of these fouling mechanisms results in a decline in the observed flow rate over time, and the decrease in filtration efficiency can be characterized by a unique signature formed by plotting the volumetric flux,  $Q$ , as a function of the total volume of fluid processed,  $V$ .

When membrane fouling takes place via any one of these mechanisms independently the QV signature is always convex downwards for filtration under a constant transmembrane pressure. However, in many such filtration scenarios, the fouling mechanisms are inherently coupled and the resulting signature is more difficult to interpret. For instance, blocking of a pore entrance will be exacerbated by the internal clogging of a pore, while the deposition of a layer of contaminants is more likely once the pores have been covered by particulates. As a result, the experimentally observed QV signature can vary dramatically from the canonical convex downwards graph, revealing features that are not captured by existing continuum models. In a range of industrially relevant cases we observe a *concave-downwards* QV signature, indicative of a fouling rate that becomes more severe with time.

This network model allows the user to explore the inter-relation between fouling mechanisms to demonstrate the impact on the QV signature.

[link to this](#)

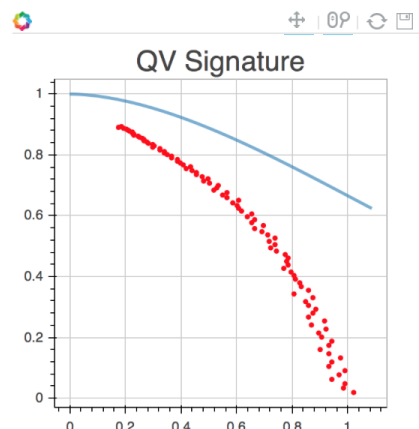
Concentration of Solution ( $c$ ): **0.604**

Adhesivity ( $k$ ): **1**

Leakage Flux ( $Q^*$ ): **0.109**

Flux at total throughput ( $Q_{min}$ ): **0.6238**

show experimental data  
 hide



## Publication

[A combined network model for membrane fouling](#), 2014, I.M. Griffiths, A. Kumar & P.S. Stewart. *J. Coll. Interf. Sci.* 432, 10.

## Network Model

Membrane fouling during particle filtration occurs through a variety of mechanisms, including internal pore clogging by contaminants, coverage of pore entrances, and deposition on the membrane surface. Each of these fouling mechanisms results in a decline in the observed flow rate over time, and the decrease in filtration efficiency can be characterized by a unique signature formed by plotting the volumetric flux,  $Q$ , as a function of the total volume of fluid processed,  $V$ .

When membrane fouling takes place via any one of these mechanisms independently the  $QV$  signature is always convex downwards for filtration under a constant transmembrane pressure. However, in many such filtration scenarios, the fouling mechanisms are inherently coupled and the resulting signature is more difficult to interpret. For instance, blocking of a pore entrance will be exacerbated by the internal clogging of a pore, while the deposition of a layer of contaminants is more likely once the pores have been covered by particulates. As a result, the experimentally observed  $QV$  signature can vary dramatically from the canonical convex downwards graph, revealing features that are not captured by existing continuum models. In a range of industrially relevant cases we observe a *concave-downwards*  $QV$  signature, indicative of a fouling rate that becomes more severe with time.

This network model allows the user to explore the inter-relation between fouling mechanisms to demonstrate the impact on the  $QV$  signature.

[link to this](#)

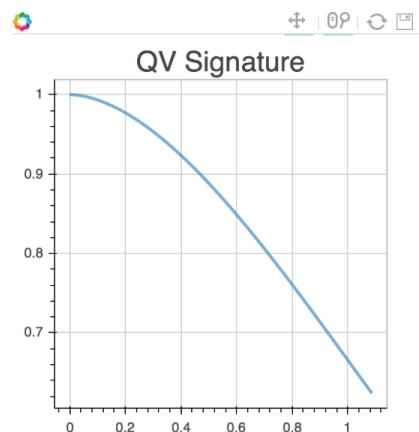
Concentration of Solution ( $c$ ): **0.604**

Adhesivity ( $k$ ): **1**

Leakage Flux ( $Q^*$ ): **0.109**

Flux at total throughput ( $Q_{min}$ ): **0.6238**

show experimental data  
 hide



## Publication

[A combined network model for membrane fouling](#), 2014, I.M. Griffiths, A. Kumar & P.S. Stewart. *J. Coll. Interf. Sci.* 432, 10.

## Network Model

Membrane fouling during particle filtration occurs through a variety of mechanisms, including internal pore clogging by contaminants, coverage of pore entrances, and deposition on the membrane surface. Each of these fouling mechanisms results in a decline in the observed flow rate over time, and the decrease in filtration efficiency can be characterized by a unique signature formed by plotting the volumetric flux,  $Q$ , as a function of the total volume of fluid processed,  $V$ .

When membrane fouling takes place via any one of these mechanisms independently the QV signature is always convex downwards for filtration under a constant transmembrane pressure. However, in many such filtration scenarios, the fouling mechanisms are inherently coupled and the resulting signature is more difficult to interpret. For instance, blocking of a pore entrance will be exacerbated by the internal clogging of a pore, while the deposition of a layer of contaminants is more likely once the pores have been covered by particulates. As a result, the experimentally observed QV signature can vary dramatically from the canonical convex downwards graph, revealing features that are not captured by existing continuum models. In a range of industrially relevant cases we observe a *concave-downwards* QV signature, indicative of a fouling rate that becomes more severe with time.

This network model allows the user to explore the inter-relation between fouling mechanisms to demonstrate the impact on the QV signature.

[link to this](#)

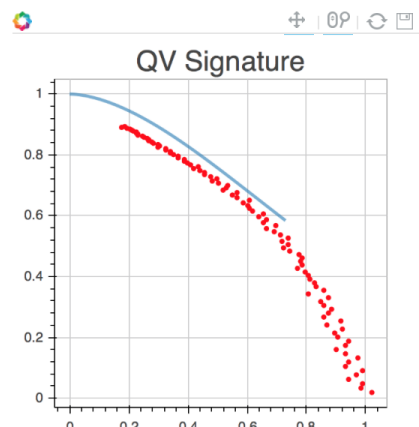
Concentration of Solution ( $c$ ): **0.9604**

Adhesivity ( $k$ ): **1**

Leakage Flux ( $Q^*$ ): **0.1288**

Flux at total throughput ( $Q_{\min}$ ): **0.5842**

show experimental data  
 hide



## Publication

[A combined network model for membrane fouling](#), 2014, I.M. Griffiths, A. Kumar & P.S. Stewart. *J. Coll. Interf. Sci.* 432, 10.

## Network Model

Membrane fouling during particle filtration occurs through a variety of mechanisms, including internal pore clogging by contaminants, coverage of pore entrances, and deposition on the membrane surface. Each of these fouling mechanisms results in a decline in the observed flow rate over time, and the decrease in filtration efficiency can be characterized by a unique signature formed by plotting the volumetric flux,  $Q$ , as a function of the total volume of fluid processed,  $V$ .

When membrane fouling takes place via any one of these mechanisms independently the QV signature is always convex downwards for filtration under a constant transmembrane pressure. However, in many such filtration scenarios, the fouling mechanisms are inherently coupled and the resulting signature is more difficult to interpret. For instance, blocking of a pore entrance will be exacerbated by the internal clogging of a pore, while the deposition of a layer of contaminants is more likely once the pores have been covered by particulates. As a result, the experimentally observed QV signature can vary dramatically from the canonical convex downwards graph, revealing features that are not captured by existing continuum models. In a range of industrially relevant cases we observe a *concave-downwards* QV signature, indicative of a fouling rate that becomes more severe with time.

This network model allows the user to explore the inter-relation between fouling mechanisms to demonstrate the impact on the QV signature.

[link to this](#)

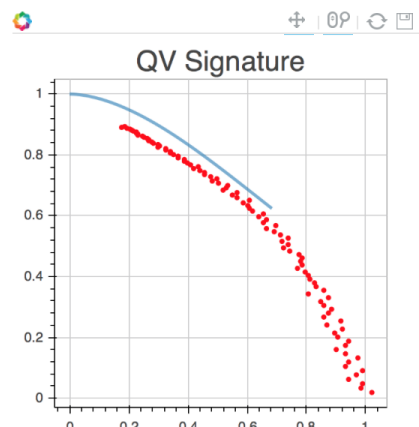
Concentration of Solution ( $c$ ): **0.9604**

Adhesivity ( $k$ ): **1**

Leakage Flux ( $Q^*$ ): **0.109**

Flux at total throughput ( $Q_{\min}$ ): **0.6238**

show experimental data  
 hide



## Publication

[A combined network model for membrane fouling](#), 2014, I.M. Griffiths, A. Kumar & P.S. Stewart. *J. Coll. Interf. Sci.* 432, 10.

